COMPARISONS BETWEEN THE BBM EQUATION AND A BOUSSINESQ SYSTEM

A. A. ALAZMAN[1,2], J. P. ALBERT[1], J. L. BONA[3], M. CHEN[4] AND J. WU[5]

[1]*Department of Mathematics, University of Oklahoma, Norman, OK 73019*
[2]*College of Sciences, Department of Mathematics, King Saud University, Riyadh, 11451, Saudi Arabia*
[3]*Department of Mathematics, Statistics and Computer Science, University of Illinois at Chicago, Chicago, IL, 60607, USA*
[4]*Department of Mathematics, Purdue University, West Lafayette, IN 47907, USA*
[5]*Department of Mathematics, Oklahoma State University, Stillwater, OK 74078*

Abstract This project aims to cast light on a Boussinesq system of equations modelling two-way propagation of surface waves. Included in the study are existence results, comparisons between the Boussinesq equations and other wave models, and several numerical simulations. The existence theory is in fact a local well-posedness result that becomes global when the solution satisfies a practically reasonable constraint. The comparison result is concerned with initial velocities and wave profiles that correspond to unidirectional propagation. In this circumstance, it is shown that the solution of the Boussinesq system is very well approximated by an associated solution of the KdV or BBM equation over a long time scale of order $\frac{1}{\epsilon}$, where ϵ is the ratio of the maximum wave amplitude to the undisturbed depth of the liquid. This result confirms earlier numerical simulations and suggests further numerical experiments which are reported here.

1. Introduction

In this report, attention will be directed to the pure initial-value problem (IVP) for a Boussinesq system of partial differential equations, namely

$$\begin{aligned} &\eta_t + v_x + \epsilon(\eta v)_x - \frac{1}{6}\epsilon\eta_{xxt} = 0, \\ &v_t + \eta_x + \epsilon v v_x - \frac{1}{6}\epsilon v_{xxt} = 0. \end{aligned} \tag{1.1}$$

The equations (1.1) are posed for $(x,t) \in \mathbb{R} \times \mathbb{R}^+$, with prescribed initial data

$$\eta(x,0) = \eta_0(x), \quad v(x,0) = v_0(x), \quad x \in \mathbb{R}. \tag{1.2}$$

This system describes approximately the propagation of certain classes of surface water waves in a uniform horizontal channel filled with an irrotational, incompressible and inviscid liquid. The dependent variables $\eta(x,t)$ and $v(x,t)$ represent the dimensionless deviation of the water surface from its undisturbed position and the horizontal velocity at the level of $\sqrt{2/3}$ of the depth of the undisturbed fluid, respectively. To make non-dimensional variables which are order-one quantities, η is scaled by a, the typical height of the waves being modelled, and v is scaled by ag/c_0, where $c_0 = \sqrt{gh_0}$, with g being the acceleration of gravity and h_0 the depth of water in its quiescent state. The coordinate x which measures distance along the channel is scaled by λ, the average wave length, and time t is scaled by λ/c_0. The small coefficient ϵ represents the ratio between the wave height a and the water depth h_0. In equation (1.1), the Stokes number $S = a\lambda^2/h_0^3$ is taken to be exactly 1 for notational simplicity. One can replace the constant $\frac{1}{6}$ by $\frac{1}{6}S$ for general values of S. In any case, it is part of the assumptions leading from the Euler equations to (1.1) that S is of order one.

One of the advantages that (1.1) has over alternative Boussinesq-type systems (see Bona, Chen & Saut [6]) is the ease with which it may be integrated numerically. In the earlier study [5], it was observed that certain solutions of the two-way models (1.1) behave very much like solutions of the unidirectional BBM model

$$q_t + q_x + \frac{3}{2}\epsilon q q_x - \frac{1}{6}\epsilon q_{xxt} = 0. \tag{1.3}$$

In this paper, a result is established showing that if the motion in the channel is properly initiated, then the solution of the Boussinesq system (1.1)-(1.2) exists and is tracked by a directly associated solution of the BBM equation (1.3) over the long time scale $\frac{1}{\epsilon}$. In light of the work of Bona, Pritchard, and Scott [8] comparing solutions of the BBM equation to solutions of the KdV equation

$$r_t + r_x + \frac{3}{2}\epsilon r r_x + \frac{1}{6}\epsilon r_{xxx} = 0, \tag{1.4}$$

this result is equivalent to a comparison between solutions of (1.1) and (1.4) (see Theorems 3.1 and 3.4 below).

Our analysis begins with a study of the well-posedness of the initial-value problem (1.1)-(1.2). An informal interpretation of the principal result is that as long as the channel bed does not run dry, the solution continues to exist. A technical description of this result will appear in Section 2.

The statement and proof of the main comparison result are given in Section 3. This section also contains a brief discussion of the resemblance between this result and others which have appeared in the recent literature (e.g., Schneider and Wayne [18]).

Motivated by the theory developed in Section 3, accurate numerical experiments are reported in Section 4. These are used to further illuminate the relation between the Boussinesq system and the BBM equation.

The paper closes with a brief conclusion which provides an appreciation of the present development and indications of interesting related lines of investigation.

2. Well-posedness results

We begin with a précis of the notation to be used in the technical sections of the paper.

For $1 \leq p < \infty$, the space of equivalence classes of Lebesgue measurable, p^{th}-power integrable, real-valued functions of a real variable is denoted L_p. The usual modification is in effect for $p = \infty$. The norm on L_p is written as $\|\cdot\|_{L_p}$. For $f \in L_2$, the Fourier transform $\widehat{f}$ of f is defined as

$$\widehat{f}(k) = \int_{-\infty}^{\infty} e^{-ikx} f(x)\, dx.$$

For $s \geq 0$, the L_2-based Sobolev class H^s is the subspace of those L_2 functions whose derivatives up to order s all lie in L_2, and the norm on H^s is given by

$$\|f\|_s^2 = \int_{-\infty}^{\infty} (1+k^2)^s |\widehat{f}(k)|^2\, dk.$$

For non-negative integers m, C_b^m is the space of m-times continuously differentiable, real-valued functions of a real variable whose derivatives up to order m are bounded on $\mathbb{R}$. The norm is

$$\|f\|_{C_b^m} = \sup_{x\in\mathbb{R}} \sum_{0\leq j\leq m} |f^{(j)}(x)|.$$

For any Banach space X and $T > 0$, $C(0,T;X)$ is the class of continuous functions from $[0,T]$ to X. If $X = L_2$, we write $\mathcal{L}_T$ for $C(0,T;L_2)$. Similarly, we write $\mathcal{B}_T^k$ for $C(0,T;C_b^k)$ and $\mathcal{H}_T^k$ for $C(0,T;H^k), k = 1, 2, \cdots$. Of course, $\mathcal{H}_T^0 = \mathcal{L}_T$. If X and Y are Banach spaces, then their Cartesian product $X \times Y$ is a Banach space with norm defined by $\|(f,g)\|_{X\times Y} = \|f\|_X + \|g\|_Y$.

Attention is now turned to the well-posedness theory. The principal result is the following.

Theorem 2.1.

(i) Let $(\eta_0, v_0) \in H^k \times H^k$, where $k \geq 0$. Then there exists $T > 0$, depending only on $\|(\eta_0, v_0)\|_{H^k\times H^k}$, such that a solution pair $(\eta, v) \in \mathcal{H}_T^k \times \mathcal{H}_T^k$ exists for the system of integral equations (2.2) below. If $k \geq 2$, then (η, v) is a classical solution of (1.1)-(1.2). There is only one solution to (2.2) in $\mathcal{H}_T^k \times \mathcal{H}_T^k$, and the mapping that associates to initial data the corresponding solution of (2.2) is continuous.

(ii) The conclusions of (i) still hold if H^k is replaced by C_b^m, where $m \geq 0$, and $\mathcal{H}_T^k$ is replaced by $\mathcal{B}_T^m$. In this case, (η, v) is a classical solution of (1.1)-(1.2) if $m \geq 1$.

(iii) Let $T_0 \in (0, \infty]$ be the maximal existence time for the solution described in (i); i.e., T_0 is the supremum of the set of values of T for which the solution exists. If there exist numbers $\alpha > 0$ and $a \in \mathbb{R}$ such that

$$1 + \epsilon\eta(x,t) > \alpha$$

for all $x \in \mathbb{R}$ and all $t \in (a, T_0)$, then $T_0 = \infty$. Also, if there exist numbers $M \in \mathbb{R}$ and $a \in \mathbb{R}$ such that

$$\|(\eta, v)\|_{L_2 \times L_2} \leq M$$

for all $t \in (a, T_0)$, then $T_0 = \infty$.

Remark 2.2. The condition $1+\epsilon\eta > 0$, when interpreted in the original physical variables, means simply that the total water height does not reach zero, which is to say the channel does not become dry.

The proof of Theorem 2.1 is similar to the proofs given for analogous results in [3] or [5]. For completeness, however, we indicate some of the details here.

To begin, write the system (1.1) in the form

$$\begin{aligned}\left(1 - \frac{1}{6}\epsilon\partial_x^2\right)\eta_t &= -(v(1+\epsilon\eta))_x,\\ \left(1 - \frac{1}{6}\epsilon\partial_x^2\right)v_t &= -\left(\eta + \frac{\epsilon}{2}v^2\right)_x.\end{aligned}$$

Inverting the operator $\left(1 - \frac{1}{6}\epsilon\partial_x^2\right)$ subject to zero boundary conditions at infinity leads to the relations

$$\begin{aligned}\eta_t &= \mathcal{M}_\epsilon * (v(1+\epsilon\eta))_x,\\ v_t &= \mathcal{M}_\epsilon * \left(\eta + \frac{\epsilon}{2}v^2\right)_x,\end{aligned} \tag{2.1}$$

where the kernel $\mathcal{M}_\epsilon$ is defined via its Fourier transform, viz.

$$\widehat{\mathcal{M}_\epsilon}(k) = \frac{-1}{1 + \epsilon k^2/6}.$$

Direct calculation using the Residue Theorem shows that for $x \in \mathbb{R}$,

$$\mathcal{M}_\epsilon(x) = \frac{-1}{2}\sqrt{\frac{6}{\epsilon}}e^{-\sqrt{6/\epsilon}|x|}.$$

Integrating by parts in (2.1) and then integrating with respect to t over the interval $(0,t)$ yields

$$\begin{aligned} \eta(x,t) &= \eta_0(x) + \int_0^t K_\epsilon * (v(1+\epsilon\eta))\ d\tau, \\ v(x,t) &= v_0(x) + \int_0^t K_\epsilon * \left(\eta + \frac{\epsilon}{2}v^2\right) d\tau \end{aligned} \tag{2.2}$$

where

$$K_\epsilon = \frac{3}{\epsilon}(\operatorname{sgn} x)e^{-\sqrt{6/\epsilon}|x|} \quad \text{and} \quad \widehat{K_\epsilon}(k) = \frac{-ik}{1+\epsilon k^2/6}.$$

Estimates of the result of convolution with K_ϵ will be needed right away. Similar estimates of the result of convolution with $\mathcal{M}_\epsilon$ will find use later. For any $f \in H^s$ where $s \geq 0$, one has that

$$\|K_\epsilon * f\|_s \leq C\epsilon^{-\frac{1}{2}}\|f\|_s. \tag{2.3}$$

(Here and in what follows, C denotes various constants which are independent of ϵ and f). This follows from a direct computation; viz.,

$$\begin{aligned} \|K_\epsilon * f\|_s^2 &= \int_{-\infty}^{\infty} (1+k^2)^s |\widehat{K_\epsilon * f}(k)|^2\ dk \\ &= \int_{-\infty}^{\infty} |\widehat{K_\epsilon}(k)|^2 (1+k^2)^s |\widehat{f}|^2\ dk \leq \left(\sup_{k\in\mathbb{R}} |\widehat{K_\epsilon}(k)|^2\right) \|f\|_s^2. \end{aligned}$$

Similarly, for any $s \geq 0$ and $f \in H^s$,

$$\|\mathcal{M}_\epsilon * f\|_s \leq C\|f\|_s. \tag{2.4}$$

In particular, if one is willing to sacrifice smoothness, then (2.4) implies that

$$\|K_\epsilon * f\|_s \leq C\|f\|_{s+1}.$$

Furthermore, for any $f, g \in L_2$, Young's inequality gives

$$\|K_\epsilon * (fg)\|_{L_2} \leq \|K_\epsilon\|_{L_2}\|fg\|_{L_1} \leq C\epsilon^{-3/4}\|f\|_{L_2}\|g\|_{L_2}. \tag{2.5}$$

Finally, we observe that if $f \in C_b^m$, $m \geq 0$, then $K_\epsilon * f \in C_b^m$ also, and estimates analogous to (2.3) and (2.5) hold; namely,

$$\|K_\epsilon * f\|_{C_b^m} \leq \|K_\epsilon\|_{L_1}\|f\|_{C_b^m} \leq C\epsilon^{-\frac{1}{2}}\|f\|_{C_b^m} \tag{2.6}$$

and

$$\|K_\epsilon * (fg)\|_{C_b^m} \leq \|K_\epsilon\|_{L_1}\|fg\|_{C_b^m} \leq C\epsilon^{-\frac{1}{2}}\|f\|_{C_b^m}\|g\|_{C_b^m}. \tag{2.7}$$

These are easily established by differentiating under the integral which defines $K_\epsilon * f$.

The proof of part (i) of Theorem 2.1 will now be considered. Let $T > 0$ be arbitrary for the moment, and write the pair of integral equations (2.2) symbolically as $(\eta, v) = A(\eta, v)$, where A is the obvious mapping of functions defined on $\mathbb{R} \times [0, T]$. It will be shown that the mapping A is contractive on a suitable subset of $\mathcal{L}_T \times \mathcal{L}_T$. Indeed, take any two elements (η_1, v_1) and (η_2, v_2) from $\mathcal{L}_T \times \mathcal{L}_T$, and notice that

$$\begin{aligned}\|A(\eta_1, v_1) - A(\eta_2, v_2)\|_{\mathcal{L}_T \times \mathcal{L}_T} \\ = \left\| \int_0^t K_\epsilon * (v_1 - v_2 + \epsilon(\eta_1 v_1 - \eta_2 v_2)) d\tau \right\|_{\mathcal{L}_T} \\ + \left\| \int_0^t K_\epsilon * (\eta_1 - \eta_2 + \frac{1}{2}\epsilon(v_1^2 - v_2^2)) d\tau \right\|_{\mathcal{L}_T}.\end{aligned}$$

Apply the basic estimates (2.3) and (2.5) to derive the inequality

$$\begin{aligned}&\|A(\eta_1, v_1) - A(\eta_2, v_2)\|_{\mathcal{L}_T \times \mathcal{L}_T} \\ &\leq CT \left[\epsilon^{-\frac{1}{2}} \|v_1 - v_2\|_{\mathcal{L}_T} + \epsilon^{\frac{1}{4}} (\|\eta_1 - \eta_2\|_{\mathcal{L}_T} \|v_1\|_{\mathcal{L}_T} + \|\eta_2\|_{\mathcal{L}_T} \|v_1 - v_2\|_{\mathcal{L}_T}) \right] \\ &\quad + CT \left[\epsilon^{-\frac{1}{2}} \|\eta_1 - \eta_2\|_{\mathcal{L}_T} + \epsilon^{\frac{1}{4}} (\|v_1\|_{\mathcal{L}_T} + \|v_2\|_{\mathcal{L}_T}) \|v_1 - v_2\|_{\mathcal{L}_T} \right] \\ &\leq CT\epsilon^{-\frac{1}{2}} \left[1 + \|(\eta_1, v_1)\|_{\mathcal{L}_T \times \mathcal{L}_T} + \|(\eta_2, v_2)\|_{\mathcal{L}_T \times \mathcal{L}_T} \right] \times \\ &\qquad \|(\eta_1, v_1) - (\eta_2, v_2)\|_{\mathcal{L}_T \times \mathcal{L}_T}.\end{aligned}$$

Suppose that both (η_1, v_1) and (η_2, v_2) are in the closed ball B_R of radius R about the zero function in $\mathcal{L}_T \times \mathcal{L}_T$. Then, the last estimate leads to the inequality

$$\|A(\eta_1, v_1) - A(\eta_2, v_2)\|_{\mathcal{L}_T \times \mathcal{L}_T} \leq \Theta \|(\eta_1, v_1) - (\eta_2, v_2)\|_{\mathcal{L}_T \times \mathcal{L}_T} \tag{2.8}$$

where $\Theta = CT\epsilon^{-\frac{1}{2}}(1 + 2R)$. If $\Theta < 1$ and A maps B_R to itself, then the hypothesis of the contraction mapping theorem will be satisfied. By application of (2.8),

$$\|A(\eta, v)\|_{\mathcal{L}_T \times \mathcal{L}_T} \leq \Theta \|(\eta, v)\|_{\mathcal{L}_T \times \mathcal{L}_T} + \|\eta_0\|_{L_2} + \|v_0\|_{L_2} \leq \Theta R + b.$$

Thus if $b \leq (1 - \Theta)R$, then A maps B_R to itself. Choosing $R = 2b$ and $T = \frac{C}{2}\epsilon^{\frac{1}{2}}(1 + 2R)^{-1}$ gives a set B_R in $\mathcal{L}_T \times \mathcal{L}_T$ on which A is a contractive self map. This proves existence in $\mathcal{L}_T \times \mathcal{L}_T$ for some $T > 0$.

Next, observe that it follows from the definition of K_ϵ that if $f \in H^k$, then $K_\epsilon * f \in H^{k+1}$. Therefore a standard bootstrap type argument allows one to conclude that if (2.2) has a solution in $L_T \times L_T$ with initial data in $H^k \times H^k$, then the solution is in fact in $\mathcal{H}_T^k \times \mathcal{H}_T^k$.

Moreover, the continuity of the solution map follows easily from the simple dependence of the operator A on the initial data. Indeed, further analysis shows that the solution map is analytic.

The question of uniqueness is now considered. Let (η_1, v_1) and (η_2, v_2) be two solutions of (2.2) in $\mathcal{L}_T \times \mathcal{L}_T$, and let

$$(\eta, v) = (\eta_1, v_1) - (\eta_2, v_2).$$

The pair (η, v) satisfies the integral equations

$$\eta = \int_0^t K_\epsilon * (v_1 - v_2 + \epsilon(\eta_1 v_1 - \eta_2 v_2))\ d\tau,$$
$$v = \int_0^t K_\epsilon * (\eta_1 - \eta_2 + \frac{1}{2}\epsilon(v_1^2 - v_2^2))\ d\tau.$$

As in the proof of the existence result, the following estimate obtains:

$$\|(\eta, v)\|_{L_2\times L_2} \le C\epsilon^{-\frac{1}{2}} \int_0^t \Big[1 + \|(\eta_1, v_1)\|_{L_2\times L_2} + \|(\eta_2, v_2)\|_{L_2\times L_2}\Big] \cdot \|(\eta_1, v_1) - (\eta_2, v_2)\|_{L_2\times L_2}\ d\tau$$
$$\le D \int_0^t \|(\eta, v)\|_{L_2\times L_2}\ d\tau,$$

where D is independent of $t \in [0, T]$. Gronwall's Lemma then implies that $\eta = 0$ and $v = 0$ on $[0, T]$, so proving uniqueness. The proof of part (i) of the Theorem is now complete.

For part (ii), we merely note that in view of (2.6) and (2.7), the same contraction-mapping argument yields local existence for initial data in C_b^m, and the same uniqueness argument applies as well. (Note that bootstrapping does not work in the context of C_b^m, since it is not true that $f \in C_b^m$ implies $K_\epsilon * f \in C_b^{m+1}$. The necessity for bootstrapping is avoided, however, if one establishes the contraction mapping directly in C_b^m rather than in C_b^0.)

The global existence result stated in part (iii) of Theorem 2.1 depends on the invariance of the functional

$$E(t) = E(\eta, v, t) = \int_{-\infty}^{\infty} \left[\eta^2 + (1 + \epsilon\eta)v^2\right]\ dx.$$

Lemma 2.3. *Let (η, v) be a solution pair of the initial-value problem (1.1),(1.2) in $\mathcal{H}^k_T \times \mathcal{H}^k_T$, $k \geq 0$, or in $\mathcal{B}^m_T \times \mathcal{B}^m_T$, $m \geq 0$. Then $E(t) = E(0)$ for all $t \in [0, T]$.*

Proof. Assume first that (η, v) is sufficiently regular for the following formal calculations to be valid; say, $(\eta, v) \in (\mathcal{H}^1_T \times \mathcal{H}^1_T) \cap (\mathcal{B}^3_T \times \mathcal{B}^3_T)$. Multiply the first equation in (1.1) by $(\eta + \frac{1}{2}\epsilon v^2 - \frac{1}{6}\epsilon v_{xt})$ and the second by $(v + \epsilon v\eta - \frac{1}{6}\epsilon\eta_{xt})$, add them, and integrate with respect to x to reach the relation

$$\int_{-\infty}^{\infty} \left(\eta_t \left[\eta + \frac{\epsilon}{2} v^2 - \frac{1}{6}\epsilon v_{xt} \right] + v_t \left[v + \epsilon v\eta - \frac{1}{6}\epsilon\eta_{xt} \right] \right) dx$$
$$= - \int_{-\infty}^{\infty} \left(\left[\eta + \frac{\epsilon}{2} v^2 - \frac{1}{6}\epsilon v_{xt} \right] \left[v + \epsilon v\eta - \frac{1}{6}\epsilon = \eta_{xt} \right] \right)_x dx = 0.$$

Regroup the terms on the left-hand side to obtain

$$\int_{-\infty}^{\infty} \left(\frac{1}{2} \left[\eta^2 + (1 + \epsilon\eta) v^2 \right]_t - \frac{1}{6}\epsilon \left[\eta_t v_{xt} + v_t \eta_{xt} \right] \right) dx = 0. \tag{2.9}$$

Since

$$\int_{-\infty}^{\infty} \left[\eta_t v_{xt} + v_t \eta_{xt} \right] dx = \int_{-\infty}^{\infty} (\eta_t v_t)_x \, dx = 0,$$

it follows from (2.9) that

$$\frac{d}{dt} \int_{-\infty}^{\infty} \left[\eta^2 + (1 + \epsilon\eta) v^2 \right] dx = 0,$$

and hence $E(t) = E(0)$ for all $t \in [0, T]$.

Now suppose that (η, v) is, say, a solution in $\mathcal{H}^k_T \times \mathcal{H}^k_T$ with $k \geq 0$. We can approximate (η_0, v_0) by regular initial data (η_{0j}, v_{0j}) and thus obtain solutions (η_j, v_j) on $[0, T]$ to which the above calculation applies, and which, by Theorem 2.1(i), approximate (η, v) in $\mathcal{H}^k_T \times \mathcal{H}^k_T$. The desired result then follows by passing to the limit. □

Remark 2.4. The functional E, together with the functional

$$F(t) = F(\eta, v, t) = \int_{-\infty}^{\infty} \left[\eta v + \frac{\epsilon}{6} \eta_x v_x \right] dx,$$

and the obvious conserved quantities

$$\int_{-\infty}^{\infty} \eta \, dx \quad \text{and} \quad \int_{-\infty}^{\infty} v \, dx$$

comprise the only known invariants for the system (1.1). Note that one obtains the invariance of F by multiplying the first equation in (1.1) by v and the second equation in (1.1) by η, adding the results, and integrating with respect to x.

The simple idea exposed in the proof of Lemma 2.3 can also be used to obtain an invariant for a more general type of Boussinesq system.

Corollary 2.5. *Consider the following four parameter class of model equations*

$$\eta_t + u_x + (u\eta)_x + au_{xxx} - b\eta_{xxt} = 0$$

and

$$u_t + \eta_x + uu_x + c\eta_{xxx} - du_{xxt} = 0.$$

If $b = d$, then for sufficiently regular solutions (η, u), the quantity

$$G(t) = \int_{-\infty}^{\infty} \left[\eta^2 + (1+\eta)u^2 - c\eta_x^2 - au_x^2\right] dx$$

is invariant, i.e., $G(t) = G(0)$ for all $t \geq 0$.

Remark 2.6. This class of model equations was put forward by Bona, Chen and Saut [6] as approximations of the two-dimensional free surface Euler equations for the flow of an ideal, incompressible liquid. In this context, a, b, c and d are not independently specifiable parameters.

The proof of part (iii) of Theorem 2.1 now proceeds by means of the usual continuation-type argument, as follows. Suppose that $1 + \epsilon\eta > \alpha > 0$ for all $x \in \mathbb{R}$ and all $t \in (a, T_0)$. According to Lemma 2.3, for $\beta = \max\{1, \alpha^{-1}\}$, we have

$$\|\eta\|_{L_2}^2 + \|v\|_{L_2}^2 = \int_{-\infty}^{\infty} (\eta^2 + v^2)\, dx \leq \beta E(t) = \beta E(0)$$

for all $t \in (a, T_0)$. Now the local existence result stated in part (i) of the Theorem implies that if (1.1) is posed with initial data $(\eta(t_0), v(t_0))$ satisfying

$$\|\eta(t_0)\|_{L_2}^2 + \|v(t_0)\|_{L_2}^2 \leq \beta E(0),$$

then a solution persists in $L_2 \times L_2$ on the time interval $(t_0, t_0 + \delta)$, where δ depends only on $\beta E(0)$. If $T_0 < \infty$, one can choose $t_0 > \min(a, T_0 - \delta)$, and thereby obtain an extension of the solution to $[0, t_0 + \delta)$. A bootstrap argument then immediately yields that this solution is in fact in $\mathcal{H}^k_{t_0+\delta} \times \mathcal{H}^k_{t_0+\delta}$. But this contradicts the maximality of T_0. Hence we must have $T_0 = \infty$. Obviously, the same argument also shows that

$T_0 = \infty$ under the assumption that $\|(\eta, v)\|_{L_2 \times L_2}$ stays bounded near T_0.

3. The Comparison Result

It is shown in [3] that the BBM equation (1.3) with initial condition $q(x, 0) = g(x)$ has a unique global solution $q \in C([0, \infty), H^s)$ if $g \in H^s$ with $s \geq 1$. Moreover, for each $T > 0$, the correspondence $g \mapsto q$ is a continuous mapping of H^s to $C([0, T]; H^s)$ while, if $l > 0$, the correspondence $g \mapsto \partial_t^l q$ is a continuous mapping of H^s to $C([0, T]; H^{s+1})$. This result was recently improved to include the range $s \geq 0$ in [11].

The question that comes to the fore now is: under what circumstances can solutions of the Boussinesq system (1.1) be approximated using the solutions of the BBM equation? Another way of putting the question would be to ask what combination of initial data (η_0, v_0) for (1.1) generates a solution (η, v) such that η is well tracked by the solution q of the BBM equation with initial data $q(x, 0) = \eta_0$. At the lowest order, we expect that if $v_0 = -\eta_0'$, then the wave moves mainly in one direction (see the discussion in [4]). However, the analysis in the last-quoted reference suggests that this simple imposition of initial data for (1.1) would not yield a solution which agrees closely with that of the BBM equation on the time scale over which nonlinearity and dispersion can have an order-one relative effect on the wave profile. Rather, one expects to have to correct the lowest-order approximation of the relation between amplitude and velocity at higher order to see the Boussinesq system evincing truly unidirectional propagation. It turns out that the appropriate relation between the initial amplitude and velocity is given by

$$\eta(x, 0) = g(x) \quad \text{and} \quad v(x, 0) = g(x) - \frac{1}{4}\epsilon g(x)^2, \tag{3.1}$$

where g is an arbitrary function of sufficient regularity.

Indeed, solutions of the initial-value problem for the Boussinesq system closely resemble an associated solution of the BBM initial-value problem over a long time interval, as the following result shows.

Theorem 3.1. *Let $j \geq 0$ be an integer. Then for every $K > 0$, there exist constants C and D such that the following is true. Suppose $g \in H^{j+5}$ with $\|g\|_{j+5} \leq K$. Let (η, v) be the solution of the Boussinesq system (1.1), with initial data defined by (3.1), and let q be the solution of the BBM equation (1.3) with initial data $q(x,0) = g(x)$. Define w by*

$$w = q - \frac{1}{4}\epsilon q^2. \tag{3.2}$$

Then for all $\epsilon \in (0,1]$, if

$$0 \leq t \leq T = D\epsilon^{-1}, \tag{3.3}$$

then

$$\|\eta(\cdot,t) - q(\cdot,t)\|_j + \|v(\cdot,t) - w(\cdot,t)\|_j \leq C\epsilon^2 t. \tag{3.4}$$

Notice that included as part of Theorem 3.1 is the assertion that the Boussinesq system has a solution in $\mathcal{H}^s_T \times \mathcal{H}^s_T$ at least for $T = D/\epsilon$.

When combined with the basic inequality

$$\|f\|_{L^\infty} \leq \|f\|^{\frac{1}{2}}_{L_2(\mathbb{R})} \|f'\|^{\frac{1}{2}}_{L_2(\mathbb{R})},$$

valid for any $f \in H^1(\mathbb{R})$, Theorem 3.1 yields the following.

Corollary 3.2. *Let $s \geq 6$ and $j \in [0, s-6]$ be integers. Then for every $K > 0$, there exist constants C and D such that the following is true. Suppose $g \in H^s$ with $\|g\|_s \leq K$. Let (η, v) be a solution of the Boussinesq system (1.1), with initial data (1.2) defined by (3.1); let q be the solution of the BBM equation (1.3) with $q(x,0) = g(x)$; and let w be defined by (3.2). Then for all $\epsilon \in (0,1]$, if*

$$0 \leq t \leq T = D\epsilon^{-1},$$

then

$$\|\partial_x^j(\eta - q)(\cdot,t)\|_{L_\infty(\mathbb{R})} + \|\partial_x^j(v - w)(\cdot,t)\|_{L_\infty(\mathbb{R})} \leq C\epsilon^2 t.$$

Remark 3.3. This result shows that, under the stated restrictions on the initial data for (1.1), solutions of (1.1) and (1.3) agree with each other to an accuracy equaling the size of the terms which were ignored in deriving (1.1) as model equations from the Euler equations. The comparison is shown to hold on a time scale of order $1/\epsilon$, which is long enough for nonlinear and dispersive effects to have an order-one influence on the wave form.

In our discussion thus far, we have focused on the BBM equation as a model for unidirectional surface waves because it lends itself easily to the numerical investigations described below in Section 4. Formally, however, the KdV equation (1.4) is at least as valid a model for unidirectional surface waves. In fact, a comparison theorem similar to Theorem 3.1 also holds for KdV.

Theorem 3.4. *Let $j \geq 0$ be an integer. Then for every $K > 0$, there exist constants C and D such that the following is true. Suppose $g \in H^{j+5}$ with $\|g\|_{j+5} \leq K$. Let (η, v) be the solution of the Boussinesq system (1.1), with initial data defined by (3.1), and let r be the solution of the KdV equation (1.4) with initial data $r(x,0) = g(x)$. Define z by*

$$z = r - \frac{1}{4}\epsilon r^2. \tag{3.5}$$

Then for all $\epsilon \in (0,1]$, if

$$0 \leq t \leq T = D\epsilon^{-1},$$

then

$$\|\eta(\cdot,t) - r(\cdot,t)\|_j + \|v(\cdot,t) - z(\cdot,t)\|_j \leq C\epsilon^2 t. \tag{3.6}$$

Implicit in the statement of the preceding theorem is the assumption that KdV is well-posed in H^s. Although the well-posedness theory for KdV is somewhat more involved than that for BBM, global well-posedness of KdV in H^s has now been proved for values of s down to $s = 0$ and below. See for example [10, 12, 16].

The proof of Theorem 3.4 is given below in Subsections 3.1 and 3.2. Once Theorem 3.4 has been proved, one then immediately obtains Theorem 3.1 as a consequence, by virtue of the following result comparing solutions of (1.3) to those of (1.4).

Theorem 3.5. *Let $j \geq 0$ be an integer. Then for every $K > 0$ and every $D > 0$, there exists a constant $C > 0$ such that the following is true. Suppose $g \in H^{j+5}$ with $\|g\|_{j+5} \leq K$. Let q be the solution of the BBM equation (1.3) with initial data $q(x,0) = g(x)$ and let r be the solution of the KdV equation (1.4) with initial data $r(x,0) = g(x)$. Then for all $\epsilon \in (0,1]$, if*

$$0 \leq t \leq T = D\epsilon^{-1},$$

then

$$\|q(\cdot,t) - r(\cdot,t)\|_j + \epsilon\|q^2(\cdot,t) - r^2(\cdot,t)\|_j \leq C\epsilon^2 t. \tag{3.7}$$

Indeed, (3.4) follows immediately from (3.6), (3.7) and the triangle inequality, in view of the definitions of w and z. Theorem 3.5 is taken from [8], where it is proved in a different form. For the reader's convenience we indicate some of the details of the proof in the Appendix.

We remark that it is also possible to prove a comparison result for (1.3) directly, without first proving Theorem 3.4. See [1] for details.

Theorems 3.1 and 3.4 are reminiscent of some interesting recent results of Craig [13] and Schneider and Wayne [18] comparing bidirectional solutions of the full Euler water-wave problem to solutions of the unidirectional KdV equation. In these papers, the water-wave problem is treated in unscaled variables, with the long wavelength and small amplitude of solutions appearing as small parameters in the initial data, rather than in the equations themselves. In such variables, the model Boussinesq system (1.1) takes the form

$$\begin{aligned} &\tilde{\eta}_t + \tilde{v}_x + (\tilde{\eta}\tilde{v})_x - \frac{1}{6}\tilde{\eta}_{xxt} = 0 \\ &\tilde{v}_t + \tilde{\eta}_x + \tilde{v}\tilde{v}_x - \frac{1}{6}\tilde{v}_{xxt} = 0. \end{aligned} \tag{3.8}$$

After rescaling (3.8) into the variables used in the present paper, and applying Theorem 3.4, one obtains the following result.

Theorem 3.6. *Suppose $g \in H^s$ with $s \geq 6$. Then there exist constants $C > 0$ and $D > 0$ such that the following is true for all $\epsilon > 0$. Let E be the solution of*

$$E_t + \frac{3}{2}EE_x + \frac{1}{6}E_{xxx} = 0$$

with $E(x,0) = g(x)$, and let $(\tilde{\eta}, \tilde{v})$ be the solution of (3.8) with $\tilde{\eta}(x,0) = \epsilon^2 g(\epsilon x)$ and $\tilde{v}(x,0) = \epsilon^2 g(\epsilon x) - \frac{1}{4}\epsilon^4 g(\epsilon x)^2$. Then for all $t \in [0, D/\epsilon^3]$, we have

$$\begin{aligned} \|\tilde{\eta}(\cdot,t) - \epsilon^2 E(\epsilon(\cdot - t), \epsilon^3 t)\|_{L_\infty(\mathbb{R})} &\leq C\epsilon^7 t \\ \|\tilde{v}(\cdot,t) - \epsilon^2 E(\epsilon(\cdot - t), \epsilon^3 t)\|_{L_\infty(\mathbb{R})} &\leq C\epsilon^7 t. \end{aligned}$$

In particular, for all $t \in [0, D/\epsilon^3]$, we have

$$\begin{aligned} \|\tilde{\eta}(\cdot,t) - \epsilon^2 E(\epsilon(\cdot - t), \epsilon^3 t)\|_{L_\infty(\mathbb{R})} &\leq CD\epsilon^4 \\ \|\tilde{v}(\cdot,t) - \epsilon^2 E(\epsilon(\cdot - t), \epsilon^3 t)\|_{L_\infty(\mathbb{R})} &\leq CD\epsilon^4. \end{aligned} \tag{3.9}$$

This result has a form similar to that of Corollaries 1.2 and 1.5 of [18], for example, where solutions of the full water-wave problem are compared to those of KdV. Notice that the power of ϵ on the right-hand side of 3.9) is larger than that appearing in the corresponding results from [18]. However, Corollaries 1.2 and 1.5 of [18] have the advantage that they allow the constant D appearing in the time interval of comparison D/ϵ^3 to be taken arbitrarily large, if one assumes that ϵ is sufficiently small. This means that, for example, the time interval can be made long enough to include soliton interactions. By contrast, an examination of the proof of Theorem 3.4 below shows that it does not allow one to take D larger than a certain fixed number which depends on g. (We remark on the other hand that the analogous constant D in Theorem 3.5 can also be taken arbitrarily large. Thus Theorem 3.5 implies the existence of solutions of BBM which look like n-soliton interactions.)

We now turn to the proof of Theorem 3.4, which will be accomplished in two stages. In Subsection 3.1, the proof of Theorem 3.4 is considered in the case $j = 0$. The detailed analysis of this case points the way to the general case. Moreover, the general case, established in Subsection 3.2, is made by an induction argument wherein the result for $j = 0$ is the starting point.

3.1. Proof of Theorem 3.4 in the case $j = 0$

One easily verifies that r and z satisfy the equations

$$r_t + z_x + \epsilon(rz)_x - \frac{1}{6}\,\epsilon r_{xxt} = -\epsilon^2 G_1,$$
$$z_t + r_x + \epsilon z z_x - \frac{1}{6}\,\epsilon z_{xxt} = -\epsilon^2 G_2 - \epsilon^3 G_3,$$

where

$$G_1 = \frac{3}{4}\,r^2 r_x - \frac{1}{4}(r r_x)_{xx} - \frac{1}{36} r_{xxxxx},$$
$$G_2 = -\frac{1}{12}\,r r_{xxx} - \frac{1}{24}\,(r^2)_{xxt},$$
$$G_3 = -\frac{1}{8}\,r^3 r_x.$$

Interest naturally focuses upon the differences

$$m = \eta - r \quad \text{and} \quad n = v - z$$

which satisfy the equations

$$
\begin{aligned}
&m_t + n_x + \epsilon(mn)_x + \epsilon(rn)_x + \epsilon(zm)_x - \frac{1}{6}\,\epsilon m_{xxt} = \epsilon^2 G_1,\\
&n_t + m_x + \epsilon(nn_x) + \epsilon(zn)_x - \frac{1}{6}\,\epsilon n_{xxt} = \epsilon^2 G_2 + \epsilon^3 G_3.
\end{aligned}
\tag{3.10}
$$

and have initial data given by $m(x,0) \equiv n(x,0) \equiv 0$.

Multiply the first equation in (3.10) by m and the second by n, add the results, and then integrate over $\mathbb{R}\times[0,t]$. After suitable integrations by parts, there appears the formula

(3.11)

$$
\begin{aligned}
&\frac{1}{2}\int_{-\infty}^{\infty}\left[m^2 + n^2 + \frac{1}{6}\epsilon m_x^2 + \frac{1}{6}\epsilon n_x^2\right]\,dx\\
&= -\,\epsilon\int_0^t\int_{-\infty}^{\infty}\left(m(mn)_x + m(rn)_x + m(zm)_x + n^2 n_x + n(zn)_x\right)\,dx\,d\tau\\
&\quad + \epsilon^2\int_0^t\int_{-\infty}^{\infty}(mG_1 + nG_2)\,dx\,d\tau + \epsilon^3\int_0^t\int_{-\infty}^{\infty} nG_3\,dx\,d\tau.
\end{aligned}
$$

The idea is to derive from (3.11) a differential inequality that will imply the desired result via a Gronwall-type lemma. The argument put forward below for accomplishing this requires ϵ-independent bounds on r and its derivatives, as furnished by the following Lemma.

Lemma 3.7. *Let $s \geq 1$ be an integer. Then for every $K > 0$, there exists $C > 0$ such that the following is true. Suppose $g \in H^s$ with $\|g\|_s \leq K$, and let r be the solution of the KdV equation (1.4) with initial data $r(x,0) = g(x)$. Then for all $\epsilon \in (0,1]$ and all $t \geq 0$,*

$$\|r\|_s \leq C.$$

Also, for every integer k such that $1 \leq 3k \leq s$, one may further assert that

$$\|\partial_t^k r\|_{s-3k} \leq C.$$

This familiar result is a consequence of the existence of infinitely many conservation laws for KdV, together with the arguments put forward in [10]. Details are provided in the Appendix so this side issue does not distract from the main line of argument.

We remark that it follows immediately from Lemma 3.7 and (3.5) that r, z and their derivatives in x up to order 5 are bounded in L_2 norm by constants which depend only on K, and which in particular are independent of t and ϵ. In what follows, we will use this fact without further comment, denoting all occurrences of such constants by C.

Define the quantity $A(t)$ to be the square root of the integral on the left-hand side of (3.11); viz.,

$$A^2(t) = \int_{-\infty}^{\infty} \left[m^2 + n^2 + \frac{1}{6}\epsilon m_x^2 + \frac{1}{6}\epsilon n_x^2 \right] dx.$$

¿From this definition it is obvious that for all t, we have

$$\|m\|_{L_2} \le A(t) \quad \text{and} \quad \|m_x\|_{L_2} \le C\epsilon^{-\frac{1}{2}} A(t).$$

Because of the elementary estimate

$$\|m\|_{L_\infty}^2 \le \|m\|_{L_2} \|m_x\|_{L_2},$$

it then follows also that

$$\|m\|_{L_\infty} \le C\epsilon^{-\frac{1}{4}} A(t).$$

Of course, the same estimates hold for n.

Now rewrite (3.11) as

$$\frac{1}{2}A^2(t) = I_1 + I_2 + I_3 + I_4, \tag{3.12}$$

where

$$\begin{aligned}
I_1 &= -\epsilon \int_0^t \int_{-\infty}^{\infty} m(mn)_x \, dx \, d\tau = \epsilon \int_0^t \int_{-\infty}^{\infty} nmm_x \, dx \, d\tau, \\
I_2 &= -\epsilon \int_0^t \int_{-\infty}^{\infty} m(rn)_x \, dx \, d\tau = \epsilon \int_0^t \int_{-\infty}^{\infty} rnm_x \, dx \, d\tau, \\
I_3 &= -\epsilon \int_0^t \int_{-\infty}^{\infty} [m(zm)_x + n(zn)_x] \, dx \, d\tau \\
&= -\frac{\epsilon}{2} \int_0^t \int_{-\infty}^{\infty} z_x(m^2 + n^2) \, dx \, d\tau, \\
I_4 &= \epsilon^2 \int_0^t \int_{-\infty}^{\infty} (mG_1 + nG_2) \, dx \, d\tau + \epsilon^3 \int_0^t \int_{-\infty}^{\infty} nG_3 \, dx \, d\tau.
\end{aligned}$$

Three of these quantities may be easily estimated as follows:

$$I_1 \leq \epsilon \int_0^t \|n\|_{L_\infty} \|m\|_{L_2} \|m_x\|_{L_2} \, d\tau \leq C\epsilon^{\frac{1}{4}} \int_0^t A^3(\tau) \, d\tau, \tag{3.13}$$

$$I_3 \leq C\epsilon \int_0^t A^2(\tau) d\tau,$$

and

$$I_4 \leq C\epsilon^2 \int_0^t A(\tau) \, d\tau + C\epsilon^3 \int_0^t A(\tau) \, d\tau.$$

It remains to estimate I_2. This apparently simple task is complicated by the requirement of not losing a factor of $\epsilon^{\frac{1}{2}}$, as this would lead to an inferior result to that stated in the theorem. Indeed, if one were to make the obvious estimate

$$I_2 \leq C\epsilon^{\frac{1}{2}} \int_0^t A^2(\tau) \, d\tau, \tag{3.14}$$

the best one could then do using Gronwall's inequality would be to establish a close comparison on a time interval of order $\epsilon^{-\frac{1}{2}}$, rather than on the desired interval of order ϵ^{-1}. Here instead of (3.14) we will use the considerably less straightforward estimate

$$I_2 \leq C\epsilon A^2(t) + C \int_0^t \left[\epsilon^3 A(\tau) + \epsilon A^2(\tau) + \epsilon^{\frac{5}{4}} A^3(\tau) \right] \, d\tau. \tag{3.15}$$

To prove (3.15), we begin by multiplying the second equation in (3.10) by rn and integrating over $\mathbb{R} \times [0, t]$ to obtain

$$\int_0^t \int_{-\infty}^{\infty} rnm_x \, dx \, d\tau = K_1 + K_2 + K_3 + K_4 + K_5,$$

where

$$K_1 = -\int_0^t \int_{-\infty}^{\infty} rnn_t \; dx \; d\tau,$$
$$K_2 = -\epsilon \int_0^t \int_{-\infty}^{\infty} rn^2 n_x \; dx \; d\tau,$$
$$K_3 = -\epsilon \int_0^t \int_{-\infty}^{\infty} rn(zn)_x \; dx \; d\tau,$$
$$K_4 = \frac{1}{6} \, \epsilon \int_0^t \int_{-\infty}^{\infty} rnn_{xxt} \; dx \; d\tau,$$
$$K_5 = \epsilon^2 \int_0^t \int_{-\infty}^{\infty} (G_2 rn + \epsilon G_3 rn) \; dx \; d\tau.$$

To estimate K_1, integrate by parts with respect to t and use the fact that $n(x,0) \equiv 0$ to derive

$$K_1 = \frac{1}{2} \int_0^t \int_{-\infty}^{\infty} r_t n^2 \; dx \; d\tau - \frac{1}{2} \int_{-\infty}^{\infty} r(x,t) n^2(x,t) \; dx.$$

In consequence, one has that

$$|K_1| \leq C \int_0^t A^2(\tau) \; d\tau + CA^2(t). \tag{3.16}$$

For K_2, one has that

$$|K_2| \leq C\epsilon \int_0^t \|n\|_{L_\infty} \|n\|_{L_2} \|n_x\|_{L_2} \; d\tau \leq C\epsilon^{\frac{1}{4}} \int_0^t A^3(\tau) \; d\tau. \tag{3.17}$$

The third integral, K_3, may be rewritten as

$$K_3 = \frac{\epsilon}{2} \int_0^t \int_{-\infty}^{\infty} (r_x z - r z_x) n^2 \; dx \; d\tau,$$

whence one obtains

$$|K_3| \leq C\epsilon \int_0^t A^2(\tau) \; d\tau. \tag{3.18}$$

The estimate for K_5 is also straightforward; viz.,

$$|K_5| \leq C\epsilon^2 \int_0^t \|n\|_{L_2} \; d\tau \leq C\epsilon^2 \int_0^t A(\tau) \; d\tau. \tag{3.19}$$

The fourth integral K_4 is more complicated. Start by writing

$$\begin{aligned} K_4 &= -\frac{1}{6}\epsilon \int_0^t \int_{-\infty}^{\infty} (rn)_x n_{xt}\, dx\, d\tau \\ &= -\frac{1}{6}\epsilon \int_0^t \int_{-\infty}^{\infty} r n_x n_{xt}\, dx\, d\tau - \frac{1}{6}\epsilon \int_0^t \int_{-\infty}^{\infty} r_x n n_{xt}\, dx\, d\tau \\ &= K_{41} + K_{42}, \end{aligned}$$

say. Using again the fact that n vanishes at $t = 0$, we have

$$\begin{aligned} K_{41} &= -\frac{1}{6}\epsilon \int_0^t \int_{-\infty}^{\infty} \frac{1}{2} r (n_x^2)_t\, dx\, d\tau \\ &= -\frac{1}{12}\epsilon \int_{-\infty}^{\infty} r(x,t) n_x^2(x,t)\, dx + \frac{1}{12}\epsilon \int_0^t \int_{-\infty}^{\infty} r_t n_x^2\, dx\, d\tau, \end{aligned}$$

and it follows directly that

$$|K_{41}| \le CA^2(t) + C\int_0^t A^2(\tau)\, d\tau. \tag{3.20}$$

For K_{42}, integrate by parts in x to get

$$K_{42} = \frac{1}{6}\,\epsilon \int_0^t \int_{-\infty}^{\infty} r_{xx} n n_t\, dx\, d\tau + \frac{1}{6}\,\epsilon \int_0^t \int_{-\infty}^{\infty} r_x n_x n_t\, dx\, d\tau = K_{421} + K_{422}.$$

Now for K_{421}, integrate by parts with respect to t as for K_1 to reach the inequality

$$|K_{421}| \le C\epsilon^{\frac{3}{4}} A^2(t) + C\epsilon \int_0^t A^2(\tau)\, d\tau. \tag{3.21}$$

(In obtaining (3.21), one uses Lemma 3.7 to obtain a bound for $\|r_{xxt}\|$ which depends only on K.)

To obtain an effective bound on K_{422}, write the second equation in (3.10) in the form

$$n_t = K_\epsilon * (m + \frac{\epsilon}{2} n^2 + \epsilon z n) - \mathcal{M}_\epsilon * (\epsilon^2 G_2 + \epsilon^3 G_3). \tag{3.22}$$

This formulation is obtained just as for the differential-integral equations (2.1) by first inverting $(1 - \frac{\epsilon}{6}\partial_x^2)$ and then integrating the terms involving $m_x, \epsilon n n_x$ and $\epsilon(zn)_x$ by parts. Using the form (3.22) for n_t in K_{422} and applying the elementary inequalities (2.3) and (2.4) connected

to convolution with K_ϵ and $\mathcal{M}_\epsilon$, we derive that

(3.23)

$$
\begin{aligned}
|K_{422}| &\le C\epsilon \int_0^t \|n_x\|_{L_2}\|n_t\|_{L_2}\, d\tau \\
&\le C\epsilon \int_0^t \|n_x\|_{L_2}\left[\epsilon^{-\frac{1}{2}}\|m+\frac{\epsilon}{2}n^2+\epsilon zn\|_{L_2}+\epsilon^2\|G_2\|_{L_2}+\epsilon^3\|G_3\|_{L_2}\right]\, d\tau \\
&\le C\int_0^t \left[\epsilon^{\frac{5}{2}}A(\tau)+A^2(\tau)+\epsilon A^3(\tau)\right]\, d\tau.
\end{aligned}
$$

Adding the inequalities (3.20), (3.21), and (3.23) leads to the bound

$$
|K_4| \le CA^2(t) + C\int_0^t \left[\epsilon^{\frac{5}{2}}A(\tau)+A^2(\tau)+\epsilon A^3(\tau)\right]\, d\tau. \tag{3.24}
$$

Finally, putting together the estimates (3.16) for K_1, (3.17) for K_2, (3.18) for K_3, (3.19) for K_5, and (3.24) for K_4, we get the desired inequality (3.15).

Now combining (3.15) with the estimates for I_1, I_3 and I_4 obtained above, we deduce from (3.12) that for all positive ϵ small enough, say $\epsilon \in (0, \epsilon_0)$,

$$
A^2(t) \le C\int_0^t \left[\epsilon^2 A(\tau)+\epsilon A^2(\tau)+\epsilon^{\frac{1}{4}}A^3(\tau)\right]\, d\tau. \tag{3.25}
$$

Of course, once ϵ_0 is fixed, then it is easy to prove that (3.25) holds as well (with a possibly larger value of C) for all $\epsilon \ge \epsilon_0$, since (3.14) implies that

$$
I_2 \le \frac{C}{\sqrt{\epsilon_0}}\,\epsilon \int_0^t A^2(\tau)\, d\tau
$$

whenever $\epsilon \ge \epsilon_0$.

¿From (3.25) and Young's inequality, it follows that

$$
A^2(t) \le C\int_0^t \left[\epsilon^2 A(\tau)+A^3(\tau)\right]\, d\tau. \tag{3.26}
$$

The following Gronwall-type lemma now comes to our aid. The proof is standard (see, e.g., [2], Lemma 2).

Lemma 3.8. *Let $\alpha > 0$, $\beta > 0$ and $\rho > 1$ be given. Define*

$$T = \beta^{-\frac{1}{\rho}} \alpha^{(1-\rho)/\rho} \int_0^\infty (1 + x^\rho)^{-1} \, dx.$$

Then there exists a constant $M = M(\rho) > 0$, which is independent of α and β, such that for any $T_1 \in [0, T]$, if $A(t)$ is a non-negative, continuous function defined on $[0, T_1]$ satisfying $A(0) = 0$ and

$$A^2(t) \leq \int_0^t [\alpha A(\tau) + \beta A^{\rho+1}(\tau)] \, d\tau$$

for all $t \in [0, T_1]$, then

$$A(t) \leq M \alpha t$$

for all $t \in [0, T_1]$.

Applying Lemma 3.8 to (3.26) with $\alpha = C\epsilon^2$, $\beta = C$, and $\rho = 2$, we obtain that

$$A(t) \leq C\epsilon^2 t$$

for all $t \in [0, D\epsilon^{-1}]$, where D, like C, is a constant depending only on K. This in turn implies that

$$\|\eta(\cdot, t) - r(\cdot, t)\|_{L_2} + \|v(\cdot, t) - z(\cdot, t)\|_{L_2} \leq C\epsilon^2 t, \tag{3.27}$$

at least for $0 \leq t \leq D\epsilon^{-1}$, which is the advertised result when $j = 0$.

The preceding inequalities were all predicated on the existence of the solution pair (η, v) of the Boussinesq system with initial data as in (3.1) based on g. The local existence theory in Section 2 guarantees that there is such a solution at least over some positive time interval. Moreover, as long as the L_2 norms $\|\eta(\cdot, t)\|_{L_2}$ and $\|v(\cdot, t)\|_{L_2}$ remain bounded, the solution continues to persist at whatever level of regularity is afforded by the initial data, according to Theorem 2.1.

Suppose now that $g \in H^5$. According to the above calculations, we know that (3.27) holds at least for $0 \leq t < T = \min(T_0, D/\epsilon)$, where T_0 is the maximum existence time for the solution (η, v) of (1.1) with initial data as in (3.1). On the other hand, as long as (3.27) holds, the triangle inequality implies that

$$\|\eta\|_{L_2} \leq \|\eta - r\|_{L_2} + \|r\|_{L_2},$$
$$\|v\|_{L_2} \leq \|v - z\|_{L_2} + \|z\|_{L_2}.$$

Thus Lemma 3.3 and (3.27) combine to yield L_2 bounds on η and v. This in turn implies that $T_0 \geq D/\epsilon$. The proof of Theorem 3.4 in the case $j = 0$ is now complete.

3.2. Proof of Theorem 3.1 in case $j \geq 1$

In this subsection, consideration is given to comparison of (r, z) and (η, v) in the Sobolev spaces H^j, $j \geq 1$. The argument is made by induction on j, the case $j = 0$ being in hand.

Define the quantity $A_j(t)$ to be the natural generalization of the function A that appeared in Subsection 3.1; namely,

$$A_j^2(t) = \int_{-\infty}^{\infty} \sum_{k=0}^{j} \left[m_{(k)}^2 + n_{(k)}^2 + \frac{1}{6}\epsilon m_{(k+1)}^2 + \frac{1}{6}\epsilon n_{(k+1)}^2 \right] \, dx,$$

where for any integer $l \geq 0$, $m_{(l)}$ denotes $\frac{\partial^l m}{\partial x^l}$ and $n_{(l)}$ denotes $\frac{\partial^l n}{\partial x^l}$. We aim to prove that there exist C_j and D_j such that if $t \in [0, D_j\epsilon^{-1}]$ then

$$A_j(t) \leq C_j \epsilon^2 t.$$

In the previous subsection, this was proved to be true for $j = 0$. Fix $j \geq 1$ and assume the result has been proved for $j - 1$. We attempt to show that it holds for j.

Taking the j^{th} derivative of equations (3.10) with respect to x yields

$$\begin{aligned} &\partial_t m_{(j)} + n_{(j+1)} + \epsilon (mn)_{(j+1)} \\ &+ \epsilon (rn)_{(j+1)} + \epsilon (zm)_{(j+1)} - \frac{1}{6}\epsilon \partial_t m_{(j+2)} = \epsilon^2 (G_1)_{(j)} \end{aligned} \tag{3.28}$$

and

$$\begin{aligned} &\partial_t n_{(j)} + m_{(j+1)} + \epsilon (n n_x)_{(j)} \\ &+ \epsilon (zn)_{(j+1)} - \frac{1}{6}\epsilon \partial_t n_{(j+2)} = \epsilon^2 (G_2)_{(j)} + \epsilon^3 (G_3)_{(j)}. \end{aligned} \tag{3.29}$$

(Note that according to Theorem 2.1, η and v, and hence also m and n, exist and remain in H^{j+5} at least for $t \in [0, D_{j-1}\epsilon^{-1}]$, so the manipulations here are justified.) Multiply (3.28) by $m_{(j)}$ and (3.29) by $n_{(j)}$, add the results, and integrate over $\mathbb{R} \times [0, t]$ to reach the relation

$$\frac{1}{2} \int_{-\infty}^{\infty} \left[m_{(j)}^2 + n_{(j)}^2 + \frac{1}{6}\epsilon \, m_{(j+1)}^2 + \frac{1}{6}\epsilon \, n_{(j+1)}^2 \right] \, dx = I_1 + I_2 + I_3 + I_4,$$

where

$$I_1 = -\epsilon \int_0^t \int_{-\infty}^{\infty} \left[(mn)_{(j+1)} m_{(j)} + (nn_x)_{(j)} n_{(j)} \right] \, dx \, d\tau,$$

$$I_2 = -\epsilon \int_0^t \int_{-\infty}^{\infty} (rn)_{(j+1)} m_{(j)} \, dx \, d\tau,$$

$$I_3 = -\epsilon \int_0^t \int_{-\infty}^{\infty} \left[(zm)_{(j+1)} m_{(j)} + (zn)_{(j+1)} n_{(j)} \right] \, dx \, d\tau,$$

$$I_4 = \epsilon^2 \int_0^t \int_{-\infty}^{\infty} \left[(G_1)_{(j)} m_{(j)} + (G_2)_{(j)} n_{(j)} \right] \, dx \, d\tau + \epsilon^3 \int_0^t \int_{-\infty}^{\infty} (G_3)_{(j)} n_{(j)} \, dx \, d\tau.$$

Our aim is to obtain estimates for I_1 through I_4 in terms of constants C which depend only on $\|g\|_{j+5}$, and hence only on K. (In what follows, we will denote all such constants by C.) Because of the induction hypothesis, it is known that there exist constants $C_{j-1} > 0$ and $D_{j-1} > 0$, depending only on $\|g\|_{j+4}$, such that

$$\|m\|_{j-1} + \|n\|_{j-1} = \|\eta - r\|_{j-1} + \|v - z\|_{j-1} \leq C_{j-1} \epsilon^2 t$$

holds for all $t \in [0, D_{j-1}\epsilon^{-1}]$. In particular,

$$\|m\|_{j-1} + \|n\|_{j-1} \leq C_{j-1} D_{j-1} \epsilon$$

for all $t \in [0, D_{j-1}\epsilon^{-1}]$. Therefore we can write that $\|m\|_{j-1} \leq C$ and $\|n\|_{j-1} \leq C$. These estimates will be used repeatedly in the induction step.

The integrand in I_1 can be expanded into a sum of terms of the form $m_{(k)} m_{(i)} n_{(l)}$ and $n_{(k)} n_{(i)} n_{(l)}$, in which each of k, i, and l is less than or equal to $j+1$, but no two can both equal $j+1$ in any term. Therefore, arguing as we did for (3.13), we can conclude that

$$|I_1| \leq C\epsilon^{\frac{1}{4}} \int_0^t A_j^3(\tau) \, d\tau. \tag{3.30}$$

To estimate I_4, we use Hölder's inequality to obtain

$$|I_4| \leq C\epsilon^2 \int_0^t A_j(\tau) \, d\tau.$$

The term I_3 can be handled by writing

$$\begin{aligned} I_3 = &- \epsilon \int_0^t \int_{-\infty}^{\infty} \Big[z(m_{(j+1)}m_{(j)} + n_{(j+1)}n_{(j)}) \\ &+ \sum_{k=1}^{j+1} \binom{j+1}{k} z_{(k)}(m_{(j+1-k)}m_{(j)} + n_{(j+1-k)}n_{(j)}) \Big] \, dx \, d\tau \\ =&\frac{1}{2} \, \epsilon \int_0^t \int_{-\infty}^{\infty} \Big[(m_{(j)}^2 + n_{(j)}^2) z_x \, dx \, d\tau \\ &- \epsilon \int_0^t \int_{-\infty}^{\infty} \sum_{k=1}^{j+1} \binom{j+1}{k} z_{(k)}(m_{(j+1-k)}m_{(j)} + n_{(j+1-k)}n_{(j)}) \, dx \, d\tau, \end{aligned}$$

from which it is obvious that

$$|I_3| \leq C\epsilon \int_0^t A_j^2(\tau) \, d\tau.$$

It remains to estimate I_2. Multiplying equation (3.29) by $rn_{(j)}$ and integrating over $\mathbb{R} \times [0,t]$, we find that

$$\int_0^t \int_{-\infty}^{\infty} rn_{(j)}m_{(j+1)} \, dx \, d\tau = K_1 + K_2 + K_3 + K_4 + K_5, \tag{3.31}$$

where

$$\begin{aligned} K_1 &= - \int_0^t \int_{-\infty}^{\infty} rn_{(j)}\partial_t n_{(j)} \, dx \, d\tau, \\ K_2 &= -\epsilon \int_0^t \int_{-\infty}^{\infty} rn_{(j)}(nn_x)_{(j)} \, dx \, d\tau, \\ K_3 &= -\epsilon \int_0^t \int_{-\infty}^{\infty} rn_{(j)}(zn)_{(j+1)} \, dx \, d\tau, \\ K_4 &= \frac{1}{6} \, \epsilon \int_0^t \int_{-\infty}^{\infty} rn_{(j)}\partial_t n_{(j+2)} \, dx \, d\tau, \\ K_5 &= \epsilon^2 \int_0^t \int_{-\infty}^{\infty} rn_{(j)} \left((G_2)_{(j)} + \epsilon (G_3)_{(j)} \right) \, dx \, d\tau. \end{aligned}$$

Now I_2 may be written as

$$\begin{aligned} I_2 &= \epsilon \int_0^t \int_{-\infty}^{\infty} (rn)_{(j)} m_{(j+1)} \, dx \, d\tau \\ &= \epsilon \int_0^t \int_{-\infty}^{\infty} r n_{(j)} m_{(j+1)} \, dx \, d\tau \\ &\quad + \epsilon \int_0^t \int_{-\infty}^{\infty} \sum_{k=1}^{j} \binom{j}{k} r_{(k)} n_{(j-k)} m_{(j+1)} \, dx \, d\tau, \end{aligned}$$

and the last term on the right-hand side is easily seen to be bounded by

$$C\epsilon \int_0^t A_j^2(\tau) \, d\tau,$$

so the key is to obtain a bound for the integral in (3.31).

We now start estimating the summands K_1 through K_5 in (3.31). First, note that the same argument used to obtain (3.16) above gives here

$$|K_1| \le C A_j^2(t) + C \int_0^t A_j^2(\tau) \, d\tau,$$

and the same argument used to obtain (3.30) above gives

$$|K_2| \le C\epsilon^{\frac{1}{2}} \int_0^t A_j^3(\tau) \, d\tau.$$

Similarly, obvious estimates give

$$|K_3| \le C\epsilon^{\frac{1}{2}} \int_0^t A_j^2(\tau) \, d\tau$$

and

$$|K_5| \le C\epsilon^2 \int_0^t A_j(\tau) \, d\tau.$$

Attention is now turned to K_4. Integrating by parts gives

$$\begin{aligned} K_4 &= -\frac{1}{6} \, \epsilon \int_0^t \int_{-\infty}^{\infty} \left[r n_{(j+1)} \partial_t n_{(j+1)} + r_x n_{(j)} \partial_t n_{(j+1)} \right] \, dx \, d\tau \\ &= K_{41} + K_{42}. \end{aligned}$$

The integral K_{41} can be handled in the same way as K_1, to reach the estimate

$$|K_{41}| \le C A_j^2(t) + C \int_0^t A_j^2(\tau) \, d\tau.$$

The quantity K_{42} may also be handled in a way that is familiar; write

$$\begin{aligned} K_{42} &= \frac{1}{6}\,\epsilon \int_0^t \int_{-\infty}^{\infty} \left[r_{xx} n_{(j)} \partial_t n_{(j)} + r_x n_{(j+1)} \partial_t n_{(j)} \right]\, dx\, d\tau \\ &= K_{421} + K_{422}, \end{aligned}$$

and follow the same procedure given above for obtaining the estimates (3.21) and (3.23), using (3.29) to replace the term $\partial_t n_{(j)}$ in K_{422}. As a result, we obtain the estimate

$$|K_4| \le C A_j^2(t) + C \int_0^t \left[\epsilon^{\frac{5}{2}} A_j(\tau) + A_j^2(\tau) + \epsilon A_j^3 \tau \right]\, d\tau,$$

as in (3.24).

Combining the estimates for K_1 through K_5 gives

$$|K| \le C A_j^2(t) + C \int_0^t \left[\epsilon^2 A_j(\tau) + A_j^2(\tau) + \epsilon^{\frac{1}{4}} A_j^3(\tau) \right]\, d\tau,$$

from which it follows that

$$|I_2| \le C\epsilon A_j^2(t) + C \int_0^t \left[\epsilon^3 A_j(\tau) + \epsilon A_j^2(\tau) + \epsilon^{\frac{5}{4}} A_j^3(\tau) \right]\, d\tau.$$

Finally, putting together the estimates for I_1 through I_4, we obtain the analogue of (3.25); i.e.,

$$A_j^2(t) \le C \int_0^t \left[\epsilon^2 A_j(\tau) + \epsilon A_j^2(\tau) + \epsilon^{\frac{1}{4}} A_j^3(\tau) \right]\, d\tau.$$

This inequality, valid for $0 \le t \le D_{j-1}\epsilon^{-1}$, taken together with Lemma 3.8, allows the conclusion that there are constants C_j and D_j depending only on $\|g\|_{j+5}$ such that

$$A_j(t) \le C_j \epsilon^2 t \quad \text{for} \quad 0 \le t \le D_j \epsilon^{-1}.$$

Thus the proof of Theorem 3.4 is complete.

4. Numerical Results

The theoretical results established in Section 3 are augmented by a numerical study reported in the present section. There are several issues of both theoretical and practical importance that are especially illuminated by numerical simulations. First, one would like an idea of

how large are the various constants that depend upon the initial data $\|g\|$. They are independent of ϵ for $\epsilon \in (0, 1]$, but if, for example, the constant D in Theorem 3.1 is some enormous multiple of the norm of the initial data, then the result has correspondingly less value. Next, it is to be expected that if only small values of ϵ are considered then the values of the constants can be improved, and presumably take on an asymptotic best value as ϵ approaches zero. An important question then is to understand just how small must ϵ be in order for the constants to approximate well their asymptotic values. A related question is whether the comparison estimate (3.4) is sharp in the sense that ϵ^2 is the highest power of ϵ that can appear there. Finally, one might ask whether the time interval of comparison in (3.3) can be extended to a longer interval, such as $[0, \epsilon^{-2}]$. Since our analytical approach casts little light on these detailed points, we have resorted to a series of numerical experiments designed to elucidate the issues.

The numerical algorithm used is based on the integral equation formulation (2.2) of (1.1) and a similar formulation of (1.3) (see [3]). The details of the numerical procedure are presented in [5] for (1.1) and [9] for (1.3). While there is no reason to report the details again here, it is worth remarking that these numerical schemes are proved to be fourth-order accurate in space and in time, to be unconditionally stable, and to have the optimal order of efficiency.

We now present and discuss the results of the numerical experiments. The first experiment, concerned with solitary waves, serves as a test of our coding in addition to continuing the conversation about the relation between (1.1) and (1.3).

Experiment 1: Solitary waves

In this experiment, we compare an exact travelling-wave solution to (1.3) with the corresponding solution of the initial-value problem for (1.1), given in Theorem (3.1). The initial data for (1.3) is taken to be

$$q(x,0) \equiv g(x) = \operatorname{sech}^2\left(\frac{1}{2}\sqrt{\frac{3}{1+\epsilon/2}}(x - x_0)\right).$$

The solution of the BBM equation corresponding to this initial data is the exact travelling wave solution $q(x,t) = g(x-kt)$, where $k = 1+\epsilon/2$

is the phase speed. Following (3.1), we solve the system (1.1) with initial data $\eta(x,0) = g(x)$ and $v(x,0) = g(x) - \frac{1}{4}\epsilon g(x)^2$. The solution of (1.1) is approximated numerically with uniform mesh sizes, given by $\Delta x = \Delta t = \frac{1}{64}\sqrt{\epsilon}$. The presence of $\sqrt{\epsilon}$ in the determination of Δx and Δt renders them independent of ϵ in the original physical variables.

An example of the results is shown in Figure 1(a), where the surface profile $\eta(x,t)$ is plotted with $\epsilon = 0.4$ and $x_0 = 19$. The solution is very nearly a travelling wave, like the solution $q(x,t)$ of (1.3), as was to be expected from the comparison result. It does have, however, a small dispersive tail. The differences between (η, v) and (q, w) are calculated, where $w(x,t) = q(x,t) - \frac{1}{4}\epsilon q(x,t)^2$. The quantities

$$\frac{|\eta(\cdot,t) - q(\cdot,t)|_p}{|q(\cdot,t)|_p} \quad \text{and} \quad \frac{|v(\cdot,t) - w(\cdot,t)|_p}{|w(\cdot,t)|_p},$$

where $|\cdot|_p$ is the $L_p(0,L)$ norm, are plotted against time t in Figure 1(b) for $t \in [0,50]$. The top two lines are the just-displayed quantities with the L_2 norm and the other two lines (which appear to be one line because they are almost identical) are those featuring the L_∞ norm. Figure 1(b) not only verifies that the relative differences increase linearly with time t for $t < C\epsilon^{-1}$, as asserted in Theorem 3.1 and Corollary 3.2, but also demonstrates that this linear estimate is valid for larger values of t. Similar results are found in Experiments 2–4 below, indicating that the time interval appearing in (3.3) is probably not the longest possible.

The solution profiles of (1.1) and (1.3) at $t = 50$ corresponding to the initial data outlined above are plotted in Figure 2(a) which shows that $\eta(x,50)$ and $q(x,50)$ have a very similar shape. However, as one sees upon consulting Figure 1(b), the relative difference between them is almost 50%. This is clearly due to phase difference, which is to say the two equations propagate their respective travelling waves at noticeably different speeds.

This leads one to imagine a comparison between solutions modulo a phase shift, or what we will call the shape difference. For a fixed t, the phase shift is determined by first finding the mesh point x_k where $\eta(x_k,t)$ takes its maximum value, and then using a quadratic polynomial interpolating $(x_k, \eta(x_k,t))$ and the two neighboring points $(x_{k-1}, \eta(x_{k-1},t))$ and $(x_{k+1}, \eta(x_{k+1},t))$ to determine the location of the

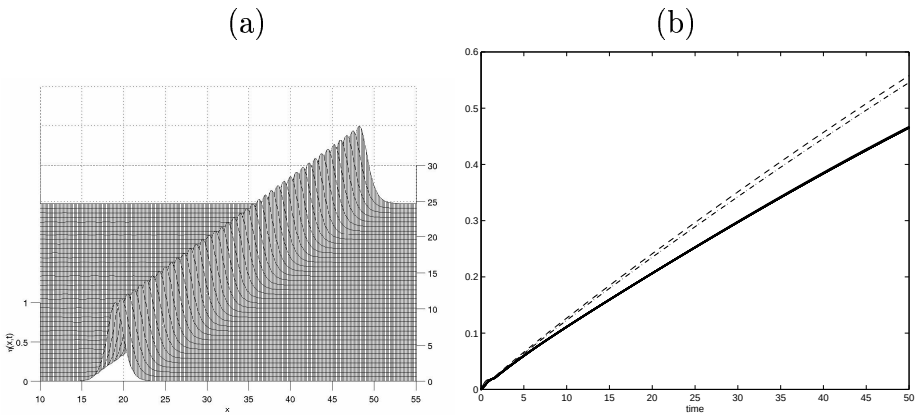

FIGURE 1. (a): Surface profile $\eta(x,t)$; (b): Relative differences between solutions of (1.1) and (1.3).

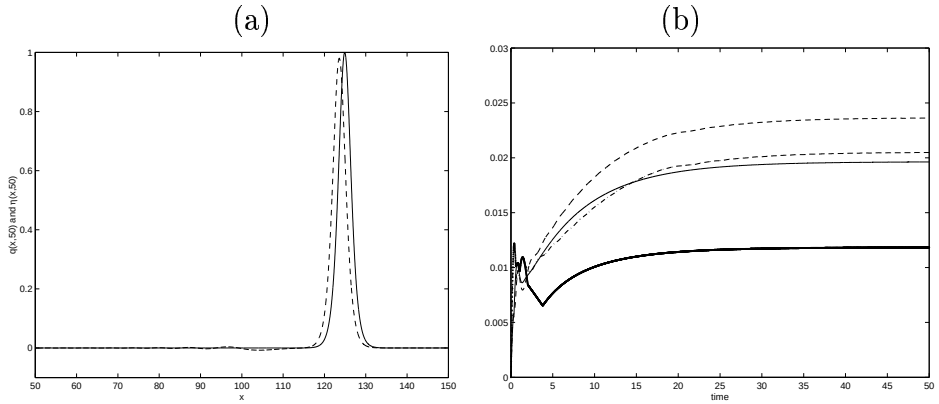

FIGURE 2. (a): A solution of (1.3) (solid line) and a corresponding solution of (1.1) (dashed line) at $t = 50$; (b): Relative shape differences between solutions of (1.3) and (1.1).

maximum point of $\eta(x,t)$; viz.,

$$x^* = \frac{(2x_k - \Delta x)\eta(x_{k+1},t) - 4x_k\eta(x_k,t) + (2x_k + \Delta x)\eta(x_{k-1},t)}{2\eta(x_{k+1},t) - 4\eta(x_k,t) - 2\eta(x_{k-1},t)}.$$

The solution $\eta^s(x,t) = \eta(x + x^* - x_0, t)$ is then compared with $g(x)$ and the relative differences calculated using the L_2 and L_∞ norms. Similarly, one can compute the relative difference between a shifted profile v^s and the initial data $v(x,0) = g - \frac{1}{4}\epsilon g^2$. The results for $\epsilon = 0.4$ are shown in Figure 2(b), where the dotted curves represent the relative shape differences for η and v calculated using the L_2 norm, and the solid lines represent the relative differences calculated using

n	1	2	3	4	5	6	7	8
ϵ_n	0.6	0.5	0.4	0.3	0.2	0.1	0.05	0.025
x_0	20	20	19	17	14	12	9	9
$\frac{\lvert\eta_\epsilon - q_\epsilon\rvert_\infty}{\lvert q_\epsilon\rvert_\infty}(\%)$	79	64	47	29	14	4.1	1.2	0.32
$\frac{\lvert v_\epsilon - w_\epsilon\rvert_\infty}{\lvert w_\epsilon\rvert_\infty}(\%)$	79	64	47	29	14	4.1	1.2	0.32
$E_2 = \frac{\lvert\eta_\epsilon - q_\epsilon\rvert_2}{\lvert q_\epsilon\rvert_2}(\%)$	98	78	56	34	17	4.6	1.3	0.34
$\frac{\lvert v_\epsilon - w_\epsilon\rvert_2}{\lvert w_\epsilon\rvert_2}$ (%)	97	76	55	34	16	4.6	1.3	0.33
rate on E_2	1.3	1.5	1.7	1.8	1.8	1.9	1.9	$\to 2$

TABLE 1. The relative difference between solutions $(\eta_\epsilon, v_\epsilon)$ of (1.1) and (q_ϵ, w_ϵ) of (1.3) at $t = 50$ and the rate of decrease of E_2 with respect to ϵ.

n	1	2	3	4	5	6	7	8
ϵ_n	0.6	0.5	0.4	0.3	0.2	0.1	0.05	0.025
x_0	20	20	19	17	14	12	9	9
$\frac{\lvert\eta^s_\epsilon - q_\epsilon\rvert_\infty}{\lvert q_\epsilon\rvert_\infty}(\%)$	3.1	2.5	2.0	1.4	0.92	0.40	0.17	0.067
$\frac{\lvert v^s_\epsilon - w_\epsilon\rvert_\infty}{\lvert w_\epsilon\rvert_\infty}(\%)$	1.5	1.4	1.2	0.97	0.71	0.37	0.17	0.066
$E^s_2 = \frac{\lvert\eta_\epsilon - q_\epsilon\rvert_2}{\lvert q_\epsilon\rvert_2}(\%)$	3.3	2.8	2.4	1.9	1.3	0.61	0.24	0.085
$\frac{\lvert v^s_\epsilon - w_\epsilon\rvert_2}{\lvert w_\epsilon\rvert_2}$ (%)	2.7	2.4	2.0	1.7	1.2	0.58	0.23	0.084
rate on E^s_2	0.83	0.82	0.83	0.90	1.1	1.3	1.5	

TABLE 2. The relative difference between solutions (q, w) of (1.3) and $(\eta^s(x,t), v^s(x,t))$, which are the shifts of solutions (η, v) of (1.1), at $t = 50$, and the rate of decrease of E^s_2 with respect to ϵ.

the L_∞ norm. The relative differences remain less that 2.5% for t up to 50.

Numerical experiments on solitary waves were conducted for other values of ϵ. To maintain the accuracy, different values of x_0 (see Table 1) were used so the solution at the boundary was consistently small over the entire temporal interval. The L_2 and L_∞ norms of the relative differences between (η, v) and (q, w) at $t = 50$ are listed in Table 1 with ϵ ranging from 0.025 to 0.6. The corresponding data on shape differences are listed in Table 2. As above, we are abbreviating the $L_2(0, L)$ and $L_\infty(0, L)$ norms by $|\cdot|_2$ and $|\cdot|_\infty$, respectively.

¿From rows 4–7 in Tables 1 and 2, one notices that the comparisons made via L_∞ or L_2 norms behave similarly. For either choice of norm, the relative error decreases as ϵ decreases, and the rates of decrease are comparable. For the rest of the discussion, therefore, we use as benchmarks the quantities

$$E_2(\epsilon,t)=\frac{|\eta_\epsilon-q_\epsilon|_2}{|q_\epsilon|_2}\quad\text{and}\quad E_2^s(\epsilon,t)=\frac{|\eta_\epsilon^s-q_\epsilon|_2}{|q_\epsilon|_2},$$

where $(\eta_\epsilon)^s$ is the solution η_ϵ after a shift matching the peaks of η_ϵ and q_ϵ.

Note that E_2 is decreasing as ϵ decreases (see row 6 in Table 1). The rate of decrease, computed by using the formula

$$\text{rate}(\epsilon_n)=\frac{\log(E_2(\epsilon_n,t)/E_2(\epsilon_{n+1},t))}{\log(\epsilon_n/\epsilon_{n+1})},$$

is shown in row 8 of Table 1. The rate of decrease is also calculated for the shape difference (see row 8 of Table 2). For relatively small ϵ, the overall difference is decreasing quadratically. The shape difference is decreasing linearly with respect to ϵ for moderate ϵ. Using Richardson extrapolation on data at $\epsilon=0.4,0.2,0.1,0.05$ and 0.025, one finds that

$$E_2(\epsilon,50)=\frac{|\eta_\epsilon-q_\epsilon|_2}{|q_\epsilon|_2}\approx 5.8\ \epsilon^2$$

as $\epsilon\to 0$. Therefore, the constant D_2 in Theorem 3.1 for $j=0$ seems to be small (about 0.12 in this example).

Comparing the data in Table 1 and Table 2, one finds that the shape difference $E_2^s(\epsilon,t)$ is much smaller than the difference $E_2(\epsilon,t)$, especially for waves of moderate size. Using a least squares approximation on data listed in row 6 of Table 2 at $\epsilon=0.6,0.5,\cdots,0.025$, one obtains

$$E_2^s(\epsilon,50)=\frac{|\eta^s-q|_2}{|q|_2}\approx 0.0494\ \epsilon.$$

We know from earlier studies (for example [7, 14]) that the solitary-wave solutions of the BBM equation play the same sort of distinguished role in the long-time asymptotics of general disturbances that they do for the Korteweg-de Vries equation. The numerical simulations in [5] show that a similar conclusion is warranted for (1.1) (and see also [17]). Consequently, it is potentially telling that an individual solitary-wave

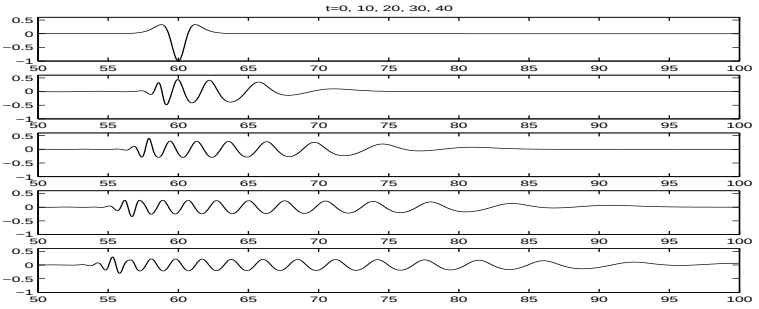

FIGURE 3. Solution of Boussinesq system with $\epsilon = 0.5$.

solution of (1.3) is seen to be very close (within 4% for all amplitudes we have tried) to solving (1.1) when the one-way velocity assumption (3.1) is imposed. Moreover, the structure of the solution of (1.1) when initiated with the BBM solitary wave appears to be a solitary-wave solution of (1.1) followed by a very small dispersive tail. Thus, the impact of the present experiment could be much broader than appears at first sight.

Experiment 2: Waves with dispersive trains

In the first experiment, the initial profile g was chosen so that it generated an exact solution of the BBM equation. However, this initial data had to depend on ϵ, albeit weakly. In the next experiment, the initial data g is fixed, independently of ϵ. We choose for this case a g that results in a lot of dispersion; namely, a profile

$$g(x) = \left(-2 + \cosh\left(3\sqrt{\frac{2}{5}}(x - x_0)\right)\right) \operatorname{sech}^4\left(\frac{3(x - x_0)}{\sqrt{10}}\right), \tag{4.1}$$

with two small crests separated by a deep trough. This profile, with $x_0 = 60$, is displayed as the top curve in Figure 3. The initial data for (1.1) is $(\eta(x,0), v(x,0)) = (g(x), g(x) - \frac{1}{4}\epsilon g^2(x))$ as before. Figure 3 shows the solution profile $\eta(x,t)$ at $t = 0, 10, 20, 30$ and 40 with $\epsilon = 0.5$. It is clear that the wave propagates to the right and also expands slowly to the left, and decays in L_∞ norm, leaving a considerable dispersive tail behind. The solution profile $q(x,t)$ of (1.3) disperses similarly (see Figure 4).

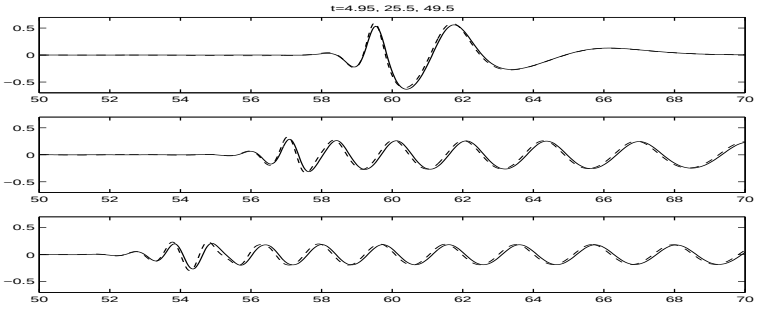

FIGURE 4. Comparison between solutions of BBM equation (solid line) and Boussinesq system (dashed line) with $\epsilon = 0.5$.

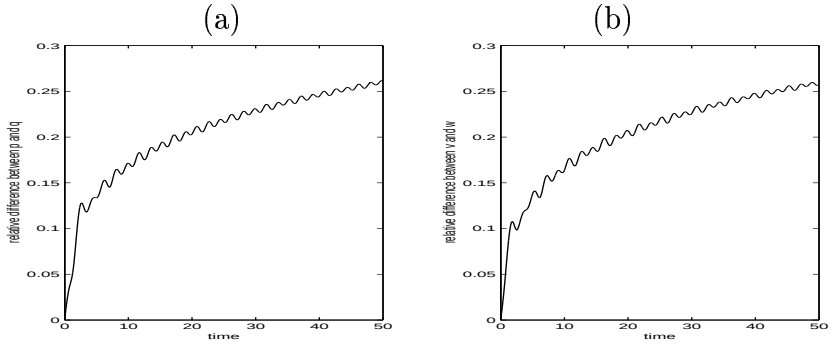

FIGURE 5. Comparison between solutions of BBM equation and Boussinesq system with $\epsilon = 0.5$, where (a) plots $\frac{|\eta - q|_2}{|q|_2}$ and (b) plots $\frac{|v-w|_2}{|w|_2}$.

The comparison between $\eta(x,t)$ and $q(x,t)$ at $t = 4.95, 25.5, 49.5$ is shown in Figure 4. It is clear that the two solutions are very close to each other. The relative differences $E_2 = \dfrac{|\eta - q|_2}{|q|_2}$ and $\tilde{E}_2 = \dfrac{|v-w|_2}{|w|_2}$ are plotted in Figure 5 for t between 0 and 50. The values of E_2 and $\tilde{E}_2$ increase relatively rapidly, but linearly, to about 10 to 12% by $t = 3$, and then more slowly thereafter. These numerical results not only verify the theoretical result $|\eta - q| \leq C\epsilon^2 t$ for $t \leq D\epsilon^{-1}$, but also demonstrate that the result may well continue to larger values of t. One sees clearly in Figure 4 that η and q have a very similar shape for all t for which the solution was calculated, but give a large value of $E_2(\epsilon, t)$ (about 26% when $t = 50$) due to the effect of a small but persistent phase shift. The data on the total differences and the shape differences are listed in Tables 3 and 4. The shape difference is calculated using a different approach because no exact solution is available. For $\alpha \in \mathbb{R}$

ϵ	0.8	0.7	0.6	0.5	0.4	0.3	0.2	0.1	0.05
$E_2 = \frac{\|\eta-q\|_2}{\|q\|_2}(\%)$	72.8	54.7	39.2	26.2	16.2	9.74	5.25	2.10	0.90
rate on E_2	2.1	2.2	2.2	2.1	1.8	1.5	1.3	1.2	
$E_2^s = \frac{\|\eta-q^s\|_2}{\|q^s\|_2}(\%)$	47.6	30.7	18.0	9.43	5.61	4.00	2.63	1.26	0.61
rate on E_2^s	3.3	3.5	3.5	2.3	1.2	1.0	1.1	1.1	

TABLE 3. The relative difference between solutions (η, v) of (1.1) and (q, w) of (1.3) at $t = 50$, with initial data (4.1) for BBM.

ϵ	0.5	0.4	0.3	0.2	0.1	0.05	0.025	0.0125
$E_2 = \frac{\|\eta-q\|_2}{\|q\|_2}(\%)$	4.3	3.3	2.4	1.4	0.51	0.18	0.053	0.015
rate on E_2	1.2	1.1	1.3	1.5	1.5	1.7	1.9	$\to 2$
$E_2^s = \frac{\|\eta-q^s\|_2}{\|q^s\|_2}(\%)$	3.71	3.03	2.30	1.39	0.501	0.173	0.052	0.014
rate on E_2^s	0.9	1.0	1.2	1.5	1.5	1.7	1.9	

TABLE 4. The relative L_2 difference between solutions $\eta(x,t)$ of (1.1) and $q(x,t)$ of (1.3) at $t = 1$, with initial data (4.1) for BBM.

and t fixed, define J to be

$$J(\alpha) = \left\{ \int_{-\infty}^{+\infty} (\eta(x,t) - q(x-\alpha,t))^2 dx \right\}^{\frac{1}{2}}$$

where $\eta(x,t)$ and $q(x,t)$ are the cubic spline interpolation functions of $\eta(x_i,t)$ and $q(x_i,t)$. The shape difference is obtained by finding the minimum value of $J(\alpha)$. The Matlab program *fminbnd* is used in our computation.

Calculations were performed with other values of ϵ and the same initial data g as above. The dependence on ϵ of the difference E_2 for ϵ equal to 0.05, 0.1, $0.2, \cdots 0.8$ is listed in Table 3. The rate of convergence to 0 degrades as ϵ approaches 0.05. Since this behavior does not match the expected asymptotic behavior as $\epsilon \to \infty$, we investigated further using values of ϵ below 0.05. The results are shown in Table 4, where one sees what looks like quadratic convergence in ϵ. These calculations were done at $t = 1$ since the t-dependence of E_2 for larger values of t is shown in Figure 5 already.

In general, for moderate sized waves, corresponding to say $\epsilon \leq 0.4$, the shape difference is small until t gets large. But for large ϵ and t, the shape difference can be large. (This is in contrast to the situation in Experiment 1, where the shape difference remained small even for large ϵ and t.) For example, for $\epsilon = 0.8$ and at $t = 50$, the shape difference is about 47.6%. A study of the wave profiles reveals the reason for this. As ϵ gets larger, the wave profile for positive time becomes more complex. There are several different amplitudes in evidence, and each of these propagates at its own speed. As the speeds in the BBM approximation are not quite the same as for the Boussinesq approximation, there is a divergence because of phase differences, just as in Experiment 1. However, because there is substantial energy in more than one wave amplitude, there may be several phase differences, so that no single translation can compensate for the phase mismatch. To put the issue in simple terms, for given functions f_1 and f_2 one cannot in general obtain a close fit to

$$f_1(x + \alpha_1) + f_2(x + \alpha_2),$$

where α_1 and α_2 are distinct, by using an approximation of the form

$$f_1(x + \alpha) + f_2(x + \alpha).$$

The solutions studied in Experiment 2 also differ from those of Experiment 1 in that their structure changes when ϵ is changed. (In Experiment 1, solutions for all values of ϵ tried had the same structure: namely, that of a solitary wave with a small dispersive tail.) The effects of changing ϵ on the solutions in Experiment 2 may be seen, for example, by comparing the solution for $\epsilon = 0.5$, shown in Figure 3, to that shown in Figure 6, where ϵ has been reduced to 0.05. In Figure 6, where $\eta(x, t)$ is graphed against x for $t = 0$, 10, 20, 30, and 40, it is clear that $\eta(x, t)$ is mainly a right-moving wave. This is in agreement with the result one gets by considering (1.1) to be a perturbation of the linear wave equations

$$\eta_t + v_x = 0$$
$$v_t + \eta_x = 0,$$

with initial conditions $\eta(x, 0) = g$ and $v(x, 0) = g - \frac{1}{4}\epsilon g^2$. For this reduced system, the analytical solution is

$$\eta(x, t) = g(x - t) + \frac{1}{8}\epsilon(g^2(x + t) - g^2(x - t))$$
$$v(x, t) = g(x - t) - \frac{1}{8}\epsilon(g^2(x + t) + g^2(x - t)),$$

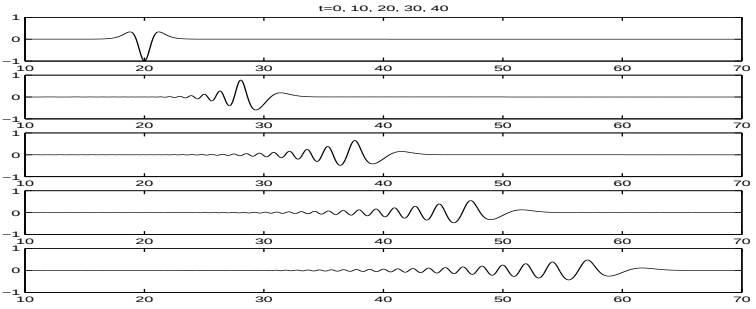

FIGURE 6. Solution of Boussinesq system with $\epsilon = 0.05$.

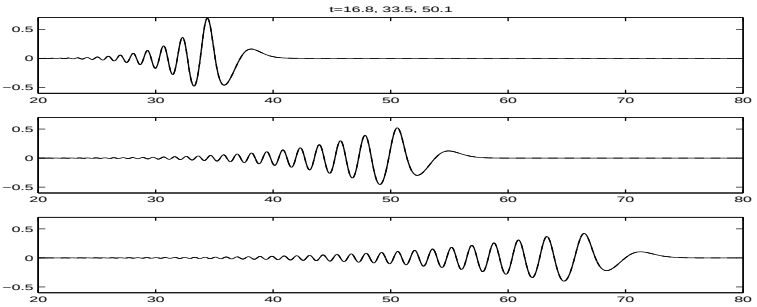

FIGURE 7. Comparison between solutions of BBM equation (solid line) and Boussinesq system (dashed line) with $\epsilon = 0.05$. The difference between the two solutions is not visible.

which to leading order is indeed a right-moving travelling wave solution.

Comparisons between $\eta(x,t)$ and $q(x,t)$ at $t = 16.8$, 33.5, and 50.1 are plotted in Figure 7. The difference between the two solutions is hardly visible. To be specific, the relative difference $E_2(0.05, 50)$ is only 0.9% at $t = 50$ (see Table 3).

As another check on our code, we monitored the variation of quantities that, for the continuous problem, are independent of time. Let $[0, L]$ denote the spatial domain used in our simulations, where $L = 360\sqrt{\epsilon}$. The integrals $I_1(t) = \int_0^L \eta(x,t)\ dx$, $I_2(t) = \int_0^L v(x,t)\ dx$, $F(t) = \int_0^L [\eta v + (\epsilon/6)\eta_x u_x]\, dx$ and $E(t) = \int_0^L [\eta^2 + v^2(1+\epsilon\eta)]\, dx$ were approximated using the trapezoidal quadrature rule applied to our numerically generated approximations. It was found that over the time interval $[0, 50]$, $I_1(t)$ was zero to within 5.9×10^{-6}, $I_2(t)$ stayed within

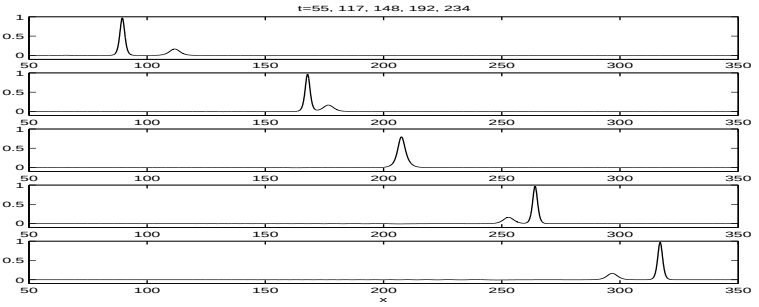

FIGURE 8. Solution of Boussinesq system.

0.008% of -0.071, $F(t)$ stayed within 0.02% of 0.43, and $E(t)$ stayed within 0.000004% of 0.51. All the computations reported here and throughout Section 4 were checked for convergence by halving the spatial and temporal grid lengths and comparing the resulting approximations.

Experiment 3: Solitary-wave interactions

In this experiment, we consider the case when a large solitary wave overtakes a small solitary wave. The initial data for the BBM equation is the superposition of two exact solitary-wave profiles; namely,

$$q(x,0) = \operatorname{sech}^2\left(\frac{1}{2}\sqrt{\frac{3}{1+0.3}}\,(x-20)\right) + \frac{1}{6}\operatorname{sech}^2\left(\frac{1}{2}\sqrt{\frac{0.5}{1+0.05}}\,(x-54)\right).$$

Numerical solution of the BBM equation with this type of initial data was carried out earlier in [7]. It was found there that two solitary-wave solutions of the BBM equation do not interact exactly (elastically), as they do in the case of the Korteweg-de Vries equation. From the results of these earlier simulations, we know that it takes a fair amount of time for the two solitary waves to fully interact. Therefore our numerical computation is carried out to $t = 234$.

The surface profiles $\eta(x,t)$ of the solutions of the Boussinesq system (1.1) with $\epsilon = 0.6$ at $t = 55, 117, 148, 192$, and 234 are shown in Figure 8. Notice how closely these profiles resemble those of a double-soliton

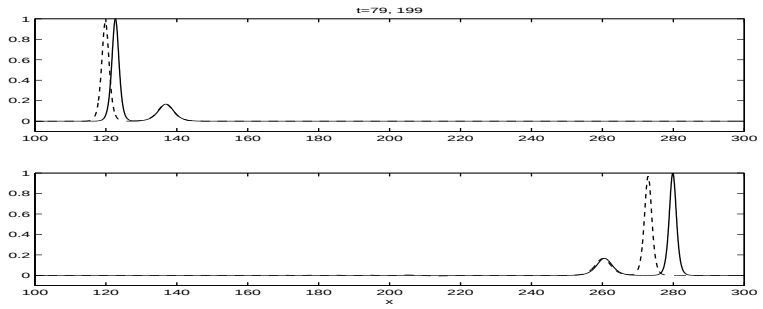

FIGURE 9. Comparison between solutions of BBM equation (solid line) and Boussinesq system (dashed line)

solution of the Korteweg-de Vries equation. Just as in a Korteweg-de Vries soliton interaction, first the large solitary wave overtakes the smaller one on account of its larger phase speed, then the two waves interact nonlinearly, and finally both emerge from the interaction having regained more or less their original shape and speed. This close resemblance between solutions of (1.1) and the Kortweg-de Vries (or BBM) equation is to be expected, for otherwise the validity of at least one of these models would be in jeopardy. It should be noted, however, that theory still falls short of being able to prove that solutions of (1.1) exhibit the behavior shown in Figure 8.

In Figure 9 are shown comparisons between the solutions of the BBM equation (1.3) and the Boussinesq system (1.1), starting from the above initial data, at $t = 79$ and 199. The phase speeds for Boussinesq solitary waves of a given amplitude are smaller than those of the BBM equation. This is especially evident for waves of larger amplitude. At $t = 199$, the phase difference for the large solitary wave has accumulated to the point where the two renditions of it differ by more than one full wavelength.

Experiment 4: Initial-boundary-value problems

In the last experiment, we attempt a simulation that corresponds to waves generated by a wavemaker in a wave tank or to regular, deep-water waves impinging upon a coast. An idealized version of this situation is to pose (1.1) or (1.3) for $(x, t) \in \mathbb{R}^+ \times \mathbb{R}^+$ with zero initial data and a sinusoidal boundary condition

$$q(0, t) = \sin(\pi t) \tanh(5t),$$

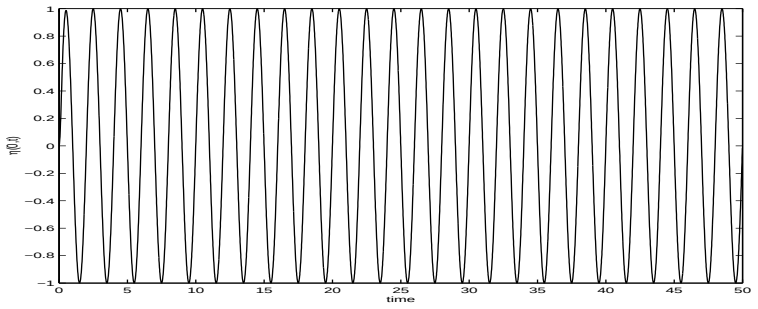

FIGURE 10. Water surface level at the wave maker.

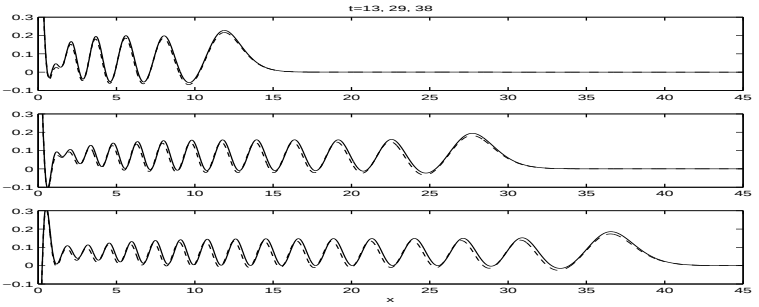

FIGURE 11. Comparison with $\epsilon = 0.2$.

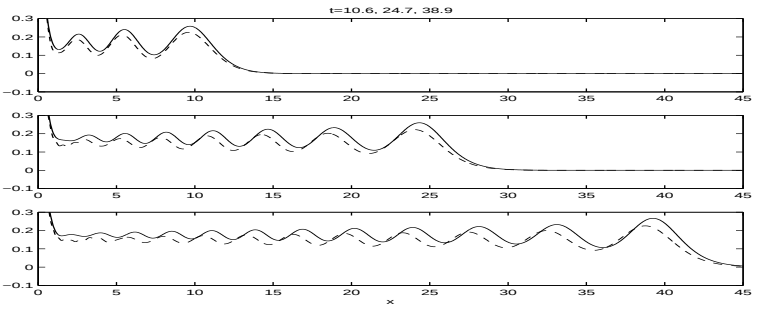

FIGURE 12. Comparison with $\epsilon = 0.5$.

which is plotted in Figure 10. The function $\tanh(5t)$ is used to ensure the compatibility of initial data and the boundary data at the corner $(x,t) = (0,0)$. The left boundary condition for the system (1.1) is taken to be $\eta(0,t) = q(0,t)$ and $v(0,t) = q(0,t) - \frac{1}{4}\epsilon q(0,t)^2$ as in (3.1).

The solutions of (1.3) and (1.1) are plotted in Figure 11 for $\epsilon = 0.2$ and in Figure 12 for $\epsilon = 0.5$. The two solutions have a similar shape, but the waves predicted by the Boussinesq system are smaller

and slower than those predicted by the BBM equation. The difference between solutions decreases as ϵ decreases.

We emphasize that no theory for comparison was developed here for such an initial-boundary-value problem. Preliminary considerations show that such a theory is not necessarily out of reach, but it is more complicated than our developments in Section 3 for comparing the pure initial-value problems.

5. Conclusions

When one attempts to model long-crested waves entering the near-shore zone of a large body of water, one naturally aims for the simplest description that is consistent with the accuracy of the input data. On the other hand, most of our knowledge of just how well various modelling approaches work derives from laboratory experiments. In both of these situations, there are available standard unidirectional models such as (1.3) or its variable-coefficient analogues which take account of variable undisturbed depth. These have been shown to predict pretty accurately in laboratory environments. There are also available more complicated systems, like (1.1) or its variable-coefficient versions, that can potentially take account of reflection. Our goal here, which had its origins in sediment transport models arising in analyzing beach protection strategies, has been to understand a precise sense in which the bidirectional model specializes to the unidirectional model. This is a fundamental question, but the answer also helps with the formulation of input to the bidirectional model in situations where we would normally have insufficient information with which to initiate the equation. In particular, records of wave-amplitude incoming from deep water are straightforward to use in initiating a unidirectional model like the BBM equation (1.3). As becomes apparent from the analysis in Section 3, the same data can be used to initiate the Boussinesq system (1.1), and with the same implied level of accuracy. The advantage is that the Boussinesq system can countenance reflection whereas (1.1) cannot. Thus, (1.1) can in principle be coupled to models for run-up and reflection in the very-near-shore zone.

In addition to presenting a qualitative theory connected with the comparison of the BBM equation and the Boussinesq system, we have reported numerical experiments showing quantitative aspects of the relation between these two models. After performing convergence tests and the like to generate confidence in our numerical scheme, we ran simulations with initial data corresponding to solitary-wave interactions and to large-scale dispersion. The results show clearly how well the Boussinesq system, with initial velocity as determined from the initial amplitude by (3.2), is tracked by the simple initial-value problem for the BBM equation. Even more convincing are the boundary-value comparisons shown in Experiment 4. As this is an important context where our ideas could come to the fore, the agreement here is heartening.

Appendix

This appendix contains the proofs of Theorem 3.5 and Lemma 3.7. For the reader's convenience, the results are restated here as Theorems A1 and A2.

Theorem A1. *Let $j \geq 0$ be an integer. Then for every $K > 0$ and every $D > 0$, there exists a constant $C > 0$ such that the following is true. Suppose $g \in H^{j+5}$ with $\|g\|_{j+5} \leq K$. Let q be the solution of the BBM equation (1.3) with initial data $q(x,0) = g(x)$ and let r be the solution of the KdV equation (1.4) with initial data $r(x,0) = g(x)$. Then for all $\epsilon \in (0,1]$, if*

$$0 \leq t \leq T = D\epsilon^{-1},$$

then

$$\|q(\cdot,t) - r(\cdot,t)\|_j + \epsilon\|q^2(\cdot,t) - r^2(\cdot,t)\|_j \leq C\epsilon^2 t.$$

Proof. This theorem is essentially proved in [8], to which we refer the reader for any details that are omitted here. First consider the case $j = 0$, and let $\theta = q - r$. Then θ satisfies the equation

$$\theta_t + \theta_x + \frac{3}{2}\epsilon(r\theta)_x + \frac{3}{2}\epsilon\theta\theta_x - \frac{1}{6}\epsilon\theta_{xxt} = \epsilon^2 G, \tag{A.1}$$

where $G = -\left(\frac{1}{4}(rr_x)_{xx} + \frac{1}{36}r_{xxxxx}\right)$. Multiplying (A.1) by θ, integrating over $\mathbb{R} \times [0,t]$, and integrating by parts leads to

$$\text{(A.2)} \quad \int_{-\infty}^{\infty} (\theta^2 + \frac{1}{6}\epsilon\theta_x^2)\ dx = \frac{3}{2}\epsilon \int_0^t r_x\theta^2\ dx\ d\tau + \epsilon^2 \int_0^t \int_{-\infty}^{\infty} G\theta\ dx\ d\tau.$$

Now let $A(t)$ be defined by setting $A^2(t)$ equal to the integral on the left side of (A.2). It follows easily from (A.2) that

$$A^2(t) \le C \int_0^t \left[\epsilon^2 A(\tau) + \epsilon A^2(\tau)\right]\ d\tau$$

where C depends only on the norm of r in H^5, and hence, by Lemma 3.7, only on K. By Gronwall's inequality it then follows that

$$A(t) \le C_1\epsilon(e^{C_2\epsilon t} - 1)$$

for all $t \ge 0$. In particular, it follows that for any $D > 0$ one can find $C > 0$ such that

$$A(t) \le C\epsilon^2 t$$

for all $t \in [0, D/\epsilon]$. Thus, for $t \in [0, D/\epsilon]$, we have $\|q - r\| \le C\epsilon^2 t$, $\|q_x - r_x\| \le C\epsilon^{3/2}t$, and

$$\begin{aligned}\|q^2 - r^2\| &= \|(q-r)(q+r)\| \le |q-r|_\infty \|q+r\| \\ &\le C\|q-r\|^{1/2}\|q_x - r_x\|^{1/2} \le C(\epsilon^2 t)^{1/2}(\epsilon^{3/2}t)^{1/2} = C\epsilon^{7/4}t.\end{aligned}$$

Therefore

$$\epsilon\|q^2 - r^2\| \le C\epsilon^{11/4}t \le C\epsilon^2 t,$$

as desired.

In case $j \ge 1$, the argument is easier: starting from (A.1) and following the procedure in Subsection 3.2 above, one obtains that the quantity $A_j(t)$ defined by

$$A_j^2(t) = \int_{-\infty}^{\infty} \sum_{k=0}^{j} \left[\theta_{(k)}^2 + \frac{1}{6}\epsilon\theta_{(k+1)}^2\right]\ dx$$

satisfies the estimate

$$A_j(t) \le C\epsilon^2 t,$$

where C depends only on K. Hence $\|q - r\|_j \le CA_j(t) \le C\epsilon^2 t$. In particular, using Lemma 3.7 we have

$$\|q + r\|_j \le \|q - r\|_j + 2\|r\|_j \le C\epsilon^2 t + C \le C$$

for all $t \in [0, D/\epsilon]$, where C depends only on K and D. Therefore, since H^j is an algebra for $j \geq 1$, we can write

$$\epsilon \|q^2 - r^2\|_j \leq C\epsilon \|q - r\|_j \|q + r\|_j \leq C\epsilon \|q - r\|_j \leq C\epsilon^3 t \leq C\epsilon^2 t,$$

as desired. □

Theorem A2. *Let $s \geq 1$ be an integer. Then for every $K > 0$, there exists $C > 0$ such that the following is true. Suppose $g \in H^s$ with $\|g\|_s \leq K$, and let r be the solution of the KdV equation (1.4) with initial data $r(x, 0) = g(x)$. Then for all $\epsilon \in (0, 1]$ and all $t \geq 0$,*

$$\|r(\cdot, t)\|_{H^s} \leq C. \tag{A.3}$$

Further, for every integer k such that $1 \leq 3k \leq s$, one may also assert that

$$\|\partial_t^j r(\cdot, t)\|_{H^{s-3k}} \leq C.$$

Proof. Define

$$\rho(x, t) = \left(\frac{3\epsilon}{2}\right) r(\sqrt{\epsilon/6}(x + t), \sqrt{\epsilon/6}\, t),$$

so that ρ is a solution of the equation

$$\rho_t + \rho\rho_x + \rho_{xxx} = 0. \tag{A.4}$$

As explained in the discussion on pp. 576–8 of [10], there exist a countable number of explicitly-defined functionals I_0, I_1, I_2, ... which are, at least formally, conserved under the flow defined by (A.4). As a consequence of the well-posedness theory of KdV presented in [10], one has that in fact $I_k(\rho)$ is independent of time for $0 \leq k \leq s$, provided $\rho \in H^s$ and $s \geq 2$. This result was later extended to $s \geq 1$ in [15].

Now the functionals I_k are defined on functions $f(x)$ by integrals of the form

$$I_k(f) = \int_{-\infty}^{\infty} P_k(f)(x)\, dx,$$

where $P_k(f)$ denotes a polynomial function of f and its derivatives. In fact, $P_k(f)$ consists of a linear combination of monomials

$$(f)^{a_0} \left(\frac{df}{dx}\right)^{a_1} \left(\frac{d^2 f}{dx^2}\right)^{a_2} \cdots \left(\frac{d^p f}{dx^p}\right)^{a_p},$$

in which the "rank" of each monomial, defined as $\sum_{i=0}^{p}(1+\frac{1}{2}i)a_i$, is equal to $k+2$. Hence if $\rho(x,t)$ and $r(x,t)$ are viewed as functions of x parameterized by the variable t, we have

$$P_k(\rho)(x,t) = \epsilon^{k+2}\tilde{P}_k(r)(\sqrt{\epsilon/6}(x+t), \sqrt{\epsilon/6}\ t)$$

for all x and t, where $\tilde{P}_k(f)$ denotes another polynomial function of f and its derivatives, which like $P_k(f)$ has coefficients which are independent of ϵ. Now define a functional $\tilde{I}_k$ by the formula

$$\tilde{I}_k(f) = \int_{-\infty}^{\infty} \tilde{P}_k(f)(x)\ dx.$$

Since $I_k(\rho)$ is independent of time, it follows that $\tilde{I}_k(r)$ is independent of time. Then the same argument as used to prove Proposition 6 of [10] allows us to conclude that the norm of r in H^s remains bounded for all time, with a bound which depends only on the H^s norm of $r(x,0) = g(x)$. Notice in particular that since the quantity ϵ does not appear in the definition of the functionals $\tilde{I}_k$, the bound thus obtained is independent of ϵ.

This proves the existence of the desired constant C in (A.3). The desired bounds on the time derivatives of r then follow immediately by using (1.4) to express time derivatives in terms of spatial derivatives. □

References

[1] A. A. Alazman, *A comparison of solutions of a Boussinesq system and the Benjamin-Bona-Mahony equation*, Ph.D. Thesis, Department of Mathematics, University of Oklahoma, Norman, OK, 2000.

[2] J. P. Albert and J. L. Bona, *Comparisons between model equations for long waves*, J. Nonlinear Sci., 1 (1991), pp. 345–374.

[3] T. B. Benjamin, J. L. Bona, and J. J. Mahony, *Model equations for long waves in nonlinear dispersive systems*, Philos. Trans. Royal Soc. London, Ser. A, 272 (1972), pp. 47–78.

[4] J. L. Bona and H. Chen, *Comparison of model equations for small-amplitude long waves*, Nonlinear Anal., 38 (1999), pp. 625–647.

[5] J. L. Bona and M. Chen, *A Boussinesq system for two-way propagation of nonlinear dispersive waves*, Physica D, 116 (1998), pp. 191–224.

[6] J. L. Bona, M. Chen, and J.-C. Saut, *Boussinesq equations and other systems for small-amplitude long waves in nonlinear dispersive media I: Derivation and the linear theory*, J. Nonlinear Sci., 12 (2002), pp. 283–318.

[7] J. L. Bona, W. G. Pritchard, and L. R. Scott, *Solitary-wave interaction*, Phys. Fluids, 23 (1980), pp. 438–441.

[8] J. L. Bona, W. G. Pritchard, and L. R. Scott, *A comparison of solutions of two model equations for long waves*, in Fluid dynamics in astrophysics and geophysics, ed. N. Lebovitz (Chicago, Ill., 1981), vol. 20 of Lectures in Appl. Math., Amer. Math. Soc., Providence, R.I., 1983, pp. 235–267.

[9] J. L. Bona, W. G. Pritchard, and L. R. Scott, *Numerical schemes for a model for nonlinear dispersive waves*, J. Comp. Physics, 60 (1985), pp. 167–186.

[10] J. L. Bona and R. Smith, *The initial-value problem for the Korteweg-de Vries equation*, Philos. Trans. Royal Soc. London, Ser. A, 278 (1975), pp. 555–601.

[11] J. L. Bona and N. Tzvetkov, *Sharp well-posedness results for the BBM-equation*, Preprint, (2002).

[12] J. Colliander, M. Keel, G. Staffilani, H. Takaoka, and T. Tao, *Sharp global well-posedness for KdV and modified KdV on R and T*, J. Amer. Math. Soc., 16 (2003), pp. 705–749

[13] W. Craig, *An existence theory for water waves, and Boussinesq and Korteweg-de Vries scaling limits*, Comm. PDE, 10 (1985), pp. 787–1003.

[14] J. C. Eilbeck and G. R. McGuire, *Numerical study of the regularized long-wave equation. II. Interaction of solitary waves*, J. Comp. Phys., 23 (1977), pp. 63–73.

[15] C. E. Kenig, G. Ponce, and L. Vega, *Well-posedness and scattering results for the generalized Korteweg-de Vries equation via the contraction principle*, Comm. Pure Appl. Math., 46 (1993), pp. 527–620.

[16] C. E. Kenig, G. Ponce, and L. Vega, *A bilinear estimate with applications to the KdV equation*, J. American Math. Soc., 9 (1996), pp. 573–603.

[17] B. Pelloni and V. A. Dougalis, *Numerical solution of some nonlocal, nonlinear dispersive wave equations*, J. Nonlinear Sci., 10 (2000), pp. 1–22.

[18] G. Schneider and C. G. Wayne, *The long-wave limit for the water wave problem. I. The case of zero surface tension*, Comm. Pure Appl. Math., 53 (2000), pp. 1475–1535.